Published in final edited form as:
Prog Retin Eye Res. 2013 July ; 35: 63–81. doi:10.1016/j.preteyeres.2013.01.005.

Adaptation of the Central Retina for High Acuity Vision: Cones, the Fovea and the Avascular Zone

Jan M Provis[a], **Adam M Dubis**[b], **Ted Maddess**[c], and **Joseph Carroll**[d]

[a]ARC Centre of Excellence in Vision Science; ANU Medical School; and John Curtin School for Medical Research, The Australian National University, Canberra, Australia

[b]Department of Ophthalmology, Duke University Eye Center, Durham, North Carolina, USA

[c]ARC Centre of Excellence in Vision Science; and John Curtin School for Medical Research, The Australian National University, Canberra, Australia

[d]Departments of Ophthalmology; Cell Biology, Neurobiology and Anatomy; and Biophysics, Medical College of Wisconsin, Milwaukee, Wisconsin, USA

Abstract

Presence of a *fovea centralis* is directly linked to molecular specification of an avascular area in central retina, before the *fovea* (or `pit') begins to form. Modeling suggests that mechanical forces, generated within the eye, initiate formation of a pit within the avascular area, and its later remodeling in the postnatal period. Within the avascular area the retina is dominated by `midget' circuitry, in which signals are transferred from a single cone to a single bipolar cell, then a single ganglion cell. Thus in inner, central retina there are relatively few lateral connections between neurons. This renders the region adaptable to tangential forces, that translocate of ganglion cells laterally / centrifugally, to form the fovea. Optical coherence tomography enables live imaging of the retina, and shows that there is greater variation in the morphology of *foveae* in humans than previously thought. This variation is associated with differences in size of the avascular area and appears to be genetically based, but can be modified by environmental factors, including prematurity. Even when the *fovea* is absent (*foveal hypoplasia*), cones in central retina adopt an elongated and narrow morphology, enabling them to pack more densely to increase the sampling rate, and to act as more effective waveguides. Given these findings, what then is the adaptive advantage of a *fovea*? We suggest that the advantages of having a pit in central retina are relatively few, and minor, but together work to enhance acuity.

Communicating Author: Prof JM Provis Jan.Provis@anu.edu.au +612 6125 4242.
[d]jcarroll@mcw.edu
[b]adam.dubis@duke.edu
[c]Ted.Maddess@anu.edu.au

[a]Fovea. Origin: Latin, meaning *small pit.* A small depression in a bone or organ. Hence `fovea centralis' is the *smallcentral pit* in the retina

[b]Marmor 2008 suggests the term `*fovea plana*' which translates as the oxymoron `flat pit'. Since the undeveloped *fovea* is an `*area centralis'* in all respects (including vascular arrangements and photoreceptor concentrations) it would be more appropriate to use this term to describe absence of a fovea.

[c]Refer to Figure 5, Van Essen, 1997

[d]Refer to Figure 1, Atchison et al., 2002

Keywords

fovea centralis; area centralis; foveal avascular zone; cone photoreceptors; axon guidance factors; antiangiogenic factors; Stiles-Crawford Effects; Fresnel numbers; visual acuity

1. Introduction

Central retina is broadly defined as the part of the retina that regards the central visual field. A useful working definition of the `central field' is the central 10° of visual angle. One degree of visual angle is imaged along approximately 0.3 mm of the human retina (Wandell, 1995). Thus the central 10° of visual field projects onto approximately the central 3 mm of retina, or a region within 1.5 mm radius of the *fovea centralis*[a] positioned at 0° eccentricity. This is a slightly larger area than the region that contains the yellow macular pigments in humans, which is 4–6° in diameter (Fawzi et al., 2011; Trieschmann et al., 2008), and is described ophthalmoscopicly as the *macula lutea* (hereafter, the macula). The *fovea centralis*, (hereafter, the fovea) is a specialization within that region, that is a depression in the surface of the retina, approximately 1.0 mm in diameter, at the centre of which is the `foveola' – where the inner retinal layers are absent and the floor of the pit is lined with the cell bodies of cone photoreceptors. The foveola approximately coincides with the area of peak cone density in the photoreceptor layer, and in general is centered within a small region devoid of retinal vessels – the `foveal avascular zone' (FAZ).

The development and function of the primate *fovea centralis* has been the subject of study and conjecture for more than one hundred years, last reviewed in 1998 (Provis et al., 1998). Since then there have been many advances in the approaches used to examine the anatomy of the *fovea* and its development, including theoretical modeling, molecular analyses and imaging technologies. A growing awareness of the significance of the FAZ in formation of the *fovea*, and the molecular mechanisms that define it has been critical. At the same time advances in *in vivo* imaging technologies have enabled visualization of the living photoreceptor mosaic, the capillary bed that defines the FAZ, as well as the morphological features of the foveal depression. These techniques, now applied to thousands of individuals, means that we now have an appreciation of the anatomical diversity of the central retina in humans, that previously was unrecognized.

Foveae feature in the retinas of many genera, but amongst mammals only in primates. However, not all primates have a *fovea*. Because we now understand that in primates, formation of a *fovea* is directly linked to specification of an avascular area, we will briefly consider the nature of central retinal specialization in afoveate species and the continuity with the primate *fovea*. The underlying theme is that central retina has evolved to enable us to see better – to resolve fine spatial detail, and colour. To this effect, the adaptations that have occurred include close packing and elongation of photoreceptors (especially cones), so-called `Midget' circuitry that dominates the macular region, and refinement and specialization of the central retinal vasculature. The drivers of these processes necessarily include biological responses to the physical properties of light. Ultimately, we aim to identify the adaptations that contribute to high visual acuity and to understand which factors contribute to our vulnerability to age-related macular degeneration.

2. Anatomy of Retinal Specializations

2.1 Streaks, *areae* and *foveae centrales*

The anatomy of neuronal populations in the mammalian retina was studied intensively in the final quarter of the twentieth century. We now understand that mammalian retinas present a

range of specializations in cell topography that are broadly associated with lifestyle (Hughes, 1977). At one extreme, plains dwelling, nocturnal species (e.g., the rabbit) tend to have high densities of ganglion cells concentrated in a horizontal band extending along the naso-temporal (anterior-posterior) axis of the retina – the *visual streak* (Hughes, 1971; Provis, 1979). At the other extreme, predatory species (e.g., cat) tend to have both photoreceptors and ganglion cells concentrated in a concentrically organized region in temporal retina, which regards the centre of the visual field – an *area centralis* (Hughes, 1975; Stone, 1978). A third group comprises mainly nocturnal, insectivorous and fruit-eating species that occupy habitats where the view is obscured by vegetation, in which the retinal specializations comprise a combination of both *visual streak* and *area centralis* (Tancred, 1981). In Strepsirrhine primates (eg., lemurs, lorises, galagos), the *area centralis* is the most common form of retinal specialization (Dkhissi-Benyahya et al., 2001; Rohen and Castenholtz, 1967; Wolin and Massopust, 1970; Woollard, 1927) while the more highly specialized homologue, the *fovea centralis*, is (amongst mammals) unique to the Haplorrhine primates (tarsiers, monkeys and apes) (Rohen and Castenholtz, 1967; Wolin and Massopust, 1970; Woollard, 1927), and found in combination with a less prominent *visual streak* in nasal retina (Stone and Johnston, 1981). The distinction between isolated `peaks' in cell density that occur in visual streaks, and the peak cell density that occurs in an *area* (and by implication, *fovea*) *centralis* has been discussed previously (Provis, 1979). In essence, peak densities of neural elements at an *area* or *fovea centralis* occur at a location that is constant within the species, is within the region of binocular overlap, regards the centre of the visual field, and is thus positioned on the `nasotemporal division' of the retina. That is, ganglion cells on the temporal side of the specialized area project to the same side of the brain, while those on the nasal side project to the opposite hemisphere (Bunt et al., 1975; Chalupa and Lia, 1991).

2.2 Adapting the retinal blood supply

Less well considered are the factors governing organization of the vasculature that supports retinal cell populations in the specialized areas. Not all mammals have a retinal blood supply (Buttery et al., 1990; Chase, 1982), the occurrence of retinal vessels being highly correlated with retinal thickness (Buttery et al., 1991). Increased retinal thickness, and in turn presence of retinal vessels, is generally associated with increased presence of cones in the outer nuclear layer (ONL. This is because the retinal circuits derived from cone photoreceptors involve less convergence onto bipolar and ganglion cells than rod pathways, so the inner nuclear layers are thicker, especially in the central region (Buttery et al., 1991). While intra-retinal vessels relieve a potential undersupply of oxygen from the outlying choroid to inner retina, they are a confounder in the complex problem of providing a clear image of the visual field to the photoreceptors – because the vessels, and the blood cells moving within them, are located between the light source and the receptor elements. Where the photoreceptor layer predominantly comprises rods, the presence of retinal vessels is unlikely to have an impact on perception of the image of the visual field striking the retina. However, in central retina where cones are closely spaced and retinal vessels form shadows that fall across adjacent cones in the array, vessels can form images that are superimposed on the image formed by the lens, causing `angioscotomas'. Studies of squirrel monkey visual system using cytochrome oxidase staining, show that retinal vessels emerging from the optic disc are represented in striate cortex, and in that retinal blood vessels separated by as little a 0.65 degrees are resolvable (Adams and Horton, 2003; Horton and Adams, 2000).

Mammalian retinas appear to have evolved a solution to this problem, which can be seen in the retina of the domestic cat - the most widely studied mammalian species with an *area centralis* (Figure 1). In the cat retina no large vessels cross the *area centralis* and only capillary-sized vessels are present in the central region (Chan-Ling et al., 1990; Henkind et

al., 1975). By minimizing the caliber of vessels crossing the photoreceptor mosaic at the *area centralis*, the risk of these structures and their contents being imaged in the cortex is removed.

The vascular structures in the retinas of the afoveate primates (the Strepsirrhini) have not been analysed in detail (to our knowledge), however, the descriptions available indicate that the arrangement of retinal vessels in the fundus of those primates closely resembles the cat (Johnson, 1901) (Rohen and Castenholtz, 1967; Wolin and Massopust, 1970; Woollard, 1927). And, in foveate, Halporrhine primates (tarsiers, monkeys and apes) the central retinal vascular specialization has evolved further such that the *fovea* is located within an FAZ (Figure 1). The significance of the relationship of the FAZ to acuity functions of the *fovea* has been discussed previously (Rodieck, 1988; Weale, 1966).

2.3 Relationship between avascular areas and presence of a fovea

Studies of foveal development in macaques and marmosets show that the FAZ is defined before the foveal depression is formed (Hendrickson et al., 2006b; Provis et al., 2000). Evidence indicates that during development, local factor/s expressed by ganglion cells at the incipient fovea prevent both the migration of astrocytes into the central area, and formation of blood vessels (Provis et al., 2000) (Kozulin et al., 2010; Kozulin et al., 2009a; Kozulin et al., 2009b). Remodeling of the capillaries surrounding the fovea takes place postnatally (Hendrickson et al., 2006b; Provis and Hendrickson, 2008), and several studies report that the diameter of the FAZ is reduced in infants born prematurely (Hammer et al., 2008; Mintz-Hittner et al., 1999; Wang et al., 2012). Available data suggests that in this group foveal diameter is unaffected by a smaller FAZ, however, other parameters including thickness of the retinal layers are found to co-vary with prematurity and size of the FAZ (Akerblom et al., 2011; Hammer et al., 2008) (Wang et al., 2012; Yanni et al., 2012), supporting the idea that modification of the vascular architecture impacts on foveal structure. Because we understand that foveal morphology is influenced both by genetic (see **4.2 Normal variation in foveal morphology – OCT**) and environmental factors like early birth, it is now important to establish consensus on which parameters can optimally measure variations in foveal morphology, so that degrees of variance attributable to genetic and environmental factors can be accurately evaluated (see **4.2 Normal variation in foveal morphology – OCT**).

Indeed, the available evidence indicates that in primates definition of the FAZ is a prerequisite for development of a *fovea*. The zoological records indicate that a *fovea* occurs only in the context of an avascular area (Wolin and Massopust, 1970). A caveat is that the nocturnal owl monkey *Aotes* has a partial, and perhaps inconsistent, *fovea* in a presumed avascular area. It has been suggested that in this species the fovea may be de-differentiating, due to the nocturnal habitat of the animal (Weale, 1966; Webb and Kaas, 1976) (Silveira et al., 1993). Alternatively, there may be a fine capillary plexus present throughout the area, not detectable through the thick ganglion cell layer; or, there may not be an adequate proportion of midget-type ganglion cells in the ganglion cell layer to permit the centrifugal displacement of cells sufficient to form a distinct foveal rim (see **3.1 The Role of Mechanical Forces**).

The best evidence of the critical role the avascular area plays in formation of the foveal depression comes from the clinical literature, using *in vivo* imaging techniques, including high resolution fluorescein angiography and optical coherence tomography (OCT). Several studies now report absence of a *fovea* (*foveal hypoplasia)* directly linked with absence of the FAZ (Azuma et al., 1996; Marmor et al., 2008; McGuire et al., 2003) and critically, there are none that report presence of a *fovea* where the FAZ is absent. The findings strongly indicate that a foveal depression does not develop in the presence of retinal vessels (see, **3.1 The**

Role of Mechanical Forces). Rather, when retinal vessels traverse the central area, the retinal specialization that forms is similar to the *area centralis* of Strepsirrhine retinas[b] (see, **4.3 Absence of the *Fovea* - OCT**).

2.4 Molecular factors define the FAZ

Identifying the factors that define the FAZ during development is key to knowing at least some of the prerequisites for formation of a *fovea*. This subject has received very little attention, even though several studies have addressed the question of differential gene expression in the *mature* foveo-macular region of the retina and pigmented epithelium (Bernstein et al., 1996; Bernstein et al., 1995; Dyer et al., 2009; Hornan et al., 2007).

Anti-angiogenic Factors

A microarray analysis of gene expression in the retina during the early phase of retinal vascular development (at 20 weeks' gestation, WG) identified 5 functional clusters of genes highly expressed at the developing macula, including a cluster of *axon guidance factors* (Kozulin et al., 2009b). Further mining of the data also showed that 3 out of 17 known *negative regulators of angiogenesis* are differentially expressed in macular samples, including the well-characterised Pigment Epithelium Derived Factor (PEDF) (Becerra et al., 2004; Karakousis et al., 2001; Kozulin et al., 2010; Spranger et al., 2001).

PEDF is expressed by ganglion cells (Karakousis et al., 2001), as well as retinal pigmented epithelial (RPE) cells, but in the developing retina PEDF is more highly expressed by ganglion cells at the incipient fovea, and in the emerging *fovea*, compared to adjacent regions of the retina (Kozulin et al., 2010). Based on its known anti-angiogenic properties (Bhutto et al., 2006; Spranger et al., 2001; Stellmach et al., 2001) it is reasonable to assume that the relatively high levels of PEDF expression at the incipient *fovea* prevent formation of retinal vessels locally, and play a key role in defining the FAZ.

Axon Guidance Factors

We carried out an analysis of the changes in the expression patterns of axon guidance factors over time. To do this, we carried out *in situ* hybridization for several guidance factors in macaque retinal sections between 55 days postconception (dPC) and 12 weeks postnatal. In each retinal section we compared levels of guidance factor expression at the macula and at a peripheral location, using the methods described for EphA6 in Kozulin et al (Kozulin et al., 2009a). Examples of our findings are shown in Figure 2. The analysis indicates that the region of peak expression of a specific factor may be different before and after birth, suggesting that the same factor plays different roles at these different stages of development (Kozulin and Provis, unpublished). Figure 2 shows that at around the time the FAZ forms (100–110 days post-conception, dPC), Unc-5h4, Netrin G1 and Eph A6 are expressed in similar ratios (macula : periphery). However, before and after this timepoint the levels of relative expression are quite different. In the early phase of gestation Netrin G1 is much more highly expressed at the macula compared to the periphery; after birth, expression levels of EphA6 are much higher in the macula compared to the periphery. This implies that in early development Netrin G1 may have a particular role in guidance of macular axons, possibly including guidance of axons away from the incipient foveal region and towards the optic disc. Such a role would be consistent with findings from small mammals indicating that Netrin/DCC interactions at the optic disc attract axons into the optic nerve (Shewan et al., 2002).

Sequential Roles for Ephrins?

A body of literature shows that the Eph/ephrin family of axon guidance factors have a role in determining the overall layout of the retinotopic map in the visual nuclei in non-primates (Huberman et al., 2008; Huberman et al., 2005). In general terms, ganglion cells expressing high levels of EphAs make connections in regions of the visual target nuclei where relatively low levels of the ephrinA ligands are expressed (McLaughlin et al., 2003a). From these `protomaps', more precise maps emerge through competition between cells for synaptic terminal field space. Some cells are eliminated, and for the remaining cells initially large synaptic territories are pruned. Studies show that gradients of such chemical factors are required to establish protomaps, and that correlated firing of ganglion cells is essential to subsequently refine the retinotopic map, to sharpen the receptive fields of ganglion cells in their visual targets, and to segregate eye-specific inputs (Eglen et al., 2003; Huberman et al., 2008; McLaughlin et al., 2003b; Pfeiffenberger et al., 2005).

In developing human retina ephrin-A5, EphA5 and EphA6 are expressed in the ganglion cell layer (Kozulin et al., 2009a; Kozulin et al., 2009b; Lambot et al., 2005). In the developing dorsal lateral geniculate nucleus (dLGN) there are complementary gradients of expression of the ligands, ephrinA5 and EphA7 where these factors likely act as substrates for eye-specific segregation (Lambot et al., 2005). In humans this process begins in the first half of gestation. Early anatomical studies show axons leaving the optic tract and entering the dorsal thalamus at 7WG, in a region that later becomes the dLGN (Cooper, 1945; Gilbert, 1935). A recent study using the lipophilic dye, DiI, shows eye-specific segregation of inputs in the dLGN at 20WG, even though differentiation of the laminae is not evident on routine inspection (Hevner, 2000). In the retina, findings in macaques (Kozulin, Natoli et al. 2009) and humans (Lambot, Depasse et al. 2005) indicate that relative levels of EphA6 are highest *temporal peripheral retina* during the first half of gestation implying a role for EphA6 in marking the input from the ipsilateral eye in the visual centres, including dLGN.

However, the relative expression of EphA6 continues to rise in the macula after the period of eye-specific segregation, becoming centred on the macula from around 100–110 dPC, and further increases in the postnatal period (Fig 2). What then is the possible role of the very high levels of EphA6 expression present at the macula *after* eye-specific segregation?

We propose two possible answers to this question. First, an hypothesis is that EphA6 expression by foveal / macular ganglion cells `advantages' them during the period of retinotopic map refinement. High levels of EphA6 may `mark' the central ganglion cells and possibly confer advantage in competition for synaptic space. Such a mechanism might ensure that ganglion cells in central retina have optimum opportunity to survive competitive interactions at the level of the dLGN, to provide generous input from the central visual field to striate cortex.

Second, it appears that EphA6 expression at the macula has an impact on the patterning of retinal blood vessels. The two ligands of EphA6 (ephrin-A1 and -A4) are expressed by migrating astrocytes in developing human and macaque retinas (Kozulin et al., 2009a). Typically, signaling between EphAs and ephrin-A receptors is *repellant*, such that high levels of Eph receptor expression repels cells that express the complementary ligand/s (Huberman et al., 2008; McLaughlin et al., 2003a). Astrocytes invade the retina at 14–15WG in humans and lead developing retinal vessels across the retina in a stereotypical pattern. They regulate proliferation of trailing endothelial cells by expressing the pro-angiogenic factor, VEGF (reviewed in (Provis, 2001)). Thus, retinal vessels do not form in regions that astrocytes do not invade. Based on this we propose that the gradient of EphA6 expression in the macula *repels astrocytes*, slowing their rate of migration towards the *fovea* and resulting in the delayed the formation of retinal vessels in the macula (reviewed in

(Provis, 2001). A critical level of EphA6 expression by foveal ganglion cells would define an astrocyte `no-go' zone.

Thus the evidence to date indicates that the FAZ is defined by the combined effects of expression gradients of both EphA6 and PEDF: first, a gradient of EphA6 expression that regulates the rate (and possibly the path) of migrating astrocytes; and second, a gradient of PEDF expression that negatively controls proliferation of endothelial cells in the foveal region.

Interestingly, the EphA6-mediated component of this process appears to `piggy-back' on a mechanism likely to have evolved primarily to establish a mapped representation of the central visual field in the brain. Expression of EphA6 ligands by astrocytes simultaneously allows for the same factor to control growth of retinal vessels in the macula and obviate the possibility of angioscotomas. It is likely that modification of the expression patterns of EphA6, PEDF and other yet unidentified factors is the cause of small FAZ associated with prematurity(Mintz-Hittner et al., 1999; Yanni et al., 2012), or absent FAZ associated with foveal hypoplasia (Azuma et al., 1996; Marmor et al., 2008; McGuire et al., 2003).

3. Formation of the *Fovea*

3.1 The role of mechanical forces – formation and remodeling

The relationship between formation of the foveal depression, and presence of the FAZ has been modeled using finite element analysis (Springer and Hendrickson, 2004a; 2004b; Springer, 1999; Springer and Hendrickson, 2005). Fundamental to this modeling is the tenet that the FAZ confers differential elasticity to the retina, since the surrounding regions have a degree of rigidity owing to the presence of the vascular network in the superficial layers, and are less responsive to mechanical forces. The mechanical forces that act on the developing retina are identified as first, a tangential force – retinal stretch - generated by ocular growth; and second, an orthogonal force generated by intraocular pressure. The modeling suggests that either intraocular pressure or retinal stretch are sufficient to generate a *fovea* in the more elastic region (Springer and Hendrickson, 2004a). However, because the foveal depression first emerges during a period when there is a relatively slow rate of ocular growth – and therefore little retinal stretch – it is concluded that the foveal depression forms just as the FAZ becomes fully defined, under the influence of intraocular pressure. The model also suggests that postnatal *remodeling* of the *fovea*, in which a narrow and deep pit becomes a wider and more shallow depression, is largely due to retinal stretch since this change coincides with a period of rapid growth of the eye (Springer and Hendrickson, 2005). This is consistent with Van Essen's proposal (1997) that tension along parallel fibres, including axons, contributes to compactness of neural circuity, and influences morphogenesis of the cortex and fovea[c].

A controversial feature of the finite element analysis model has been the suggestion that the tensile forces generated by retinal stretch also generate axial `lifting forces' that promote elongation of photoreceptors within the FAZ to mediate cone packing, or crowding, in the foveal cone mosaic (Springer, 1999; Springer and Hendrickson, 2005). However, packing of cones in the photoreceptor mosaic of central retina commences prior to definition of the avascular areas (Diaz-Araya and Provis, 1992), and in other primates cone packing in central retina is present in the absence of a *fovea* and FAZ (see below **3.2 Photoreceptor Elongation and Packing**) suggesting that other factors mediate the packing of cones in the foveal cone mosaic. Furthermore, the OCT evidence shows that many individuals lacking a *fovea* and FAZ have features in central outer retina that are consistent with normal cone packing densities, and may have visual acuity in the normal range (see **4.3 Absence of the Fovea**).

3.2 Photoreceptor elongation, crowding and packing density

Quantitative data that documents morphological adaptation of the central photoreceptors during development, has been derived from only 3 (foveate) species – human, macaque and marmoset. Relatively little is known about other primate species, particularly the Strepsirrhine (afoveate) species. However, descriptive studies suggest that elongation and accumulation of photoreceptors in the central region is a common feature (Wolin and Massopust, 1970; Woollard, 1927). In addition, semi-quantitative data from a wide range of afoveate and foveate primates is available from a study carried out by Rohen and Castenholtz (1967). Those authors examined and compared the thickness of the retinal layers at 5 standardized locations in retinae with *area centrales*, or *foveae centrales*, and represented the findings diagrammatically – some of which are shown in Figure 3. The data indicate that significant elongation and packing of photoreceptors occurs in the central area of the retina even in the absence of a *fovea* – and that the trend is stronger in some species (eg., *Lemur catta, Galego senegalensis*) than others (eg., *Indri indri*). The data from the species presented in the column to the right in Figure 3 indicate that elongation is more pronounced in the presence of a *fovea*.

Those data point to mechanism/s that mediate elongation photoreceptors and facilitate cone packing, or crowding, *in the absence of a fovea centralis*. Another line of evidence pointing in this direction is that during early development photoreceptors at the posterior pole begin to become more elongated and more tightly packed, *prior to* emergence of the early *fovea*. In humans this amounts to a change in cone density from ~14K/mm^2 at 13WG to ~28K/mm^2 by 24WG, without addition of new cells (Diaz-Araya and Provis, 1992).

We now understand that the process of packing foveal cones into the central photoreceptor mosaic is `suspended' during the early formation of the *fovea*, from around 25WG in humans (or ~110dPC in macaques) until the postnatal period. In effect maturation of the foveal region, including elongation of cones, is delayed relative to maturation of the para- and perifovea until after birth in humans, macaques and marmosets – these being the only 3 species that have been studied (Abramov et al., 1982; Cornish et al., 2005; Dubis et al., 2012a; Springer et al., 2011).

3.3 Changes in cell shape mediate increases in cone density

When cones first exit the cell cycle they are cuboidal in shape, and become columnar before the inner and outer segments emerge and lengthen in late gestation and early postnatal life (Hendrickson and Yuodelis, 1984). In late gestation foveal cones begin to elaborate a long axonal process in late gestation (fibres of Henle) then undergo elongation over a protracted period of time in the postnatal phase. During this period the differentiating cones have a very distinctive distribution of FGF receptors in different region of the cell membrane, as illustrated in Figure 4. This elongation of cones at the posterior pole, in the presence of strong cell-cell associations between neighbors, mediates the increases in cone density at the posterior pole, and in the *fovea* during early development and in the postnatal phase.

Fibroblast growth factor 2 (FGF2) is a well-known morphogenetic factor. Analysis of FGFR and FGF2 expression by cone photoreceptors in the developing macaque retina *before, during* and *after* the emergence of the early *fovea* (Fig. 4) suggests a role for FGF signaling in cone morphogenesis(Cornish et al., 2005; Cornish et al., 2004). In particular, FGF2 expression (Fig. 4) and FGFR4 expression (not shown) is elevated in foveal cones during the postnatal period when they are rapidly elongating, but is significantly down-regulated during the period that differentiation of cones in the *fovea* is suspended (Cornish et al., 2005). Expression levels of mRNA encoding FGF2 expression in ganglion cells does not vary over the same period in the same sections, indicating that these effects are specific to foveal

photoreceptors. The findings strongly suggest that elongation – and hence the packing – of cones in the central *fovea* is mediated by FGF signaling. Further exploration of the effects of FGF signaling on cone morphogenesis in murine models or zebrafish is needed to better understand these processes.

3.4 Excavation of the inner retina - the significance of `Midget' pathways

An aspect of foveal development that has not (to our knowledge) been canvassed previously is the role that the midget ganglion cell pathways located within the FAZ may play in determination of foveal morphology. The morphology of the early foveal depression is quite different from the mature depression (Fig 5). The early *fovea* is a very shallow depression in the ganglion cell layer (GCL) that is marginally thinned compared to the rim; the thicknesses of the inner plexiform and inner nuclear layers are virtually unchanged, as illustrated in Figure 5 A and B. This early form of the *fovea* transforms quite quickly into a profile that shows a dramatically thinned GCL, due to displacement of GC out of the FAZ (Fig 5C), and onto the foveal rime. This rapid change can be explained in terms of the predominance of midget circuitry within the FAZ, in which the majority of bipolar cells are `midget bipolar cells' that connect to a single cone in the ONL and a single ganglion cell in the GCL. This arrangement would allow each element of the midget output pathway (cone - bipolar cell - ganglion cell) to respond to foveogenic forces independent of its neighbors.

Because parasol cell circuits are converging, and a single parasol ganglion cells gets input from multiple `diffuse' bipolar cells they cannot be so readily displaced. In the macaque *fovea*, it is estimated that each parasol ganglion cell receives input from 30–50 cones, via 5–10 diffuse bipolar cells (Grünert et al., 1993). Hence displacement of a single parasol ganglion cell to generate a foveal depression would require rearrangement of many interconnected cells. In macaque retina parasol ganglion cells comprise about 5% of the GC population within 500μm of the central *fovea*, and those present in the foveola have large, distorted dendritic fields, suggesting that their processes have been drawn in opposing directions during formation of the depression (Grünert et al., 1993). A larger proportion of parasol cells in the central region would likely mean that larger numbers of GC stayed in the foveola.

Thus, an important factor contributing to foveal morphology is the relative proportion of midget and parasol circuits present in the FAZ. Any FAZ in which parasol cell pathways were predominant would probably have a depression with an intact GCL, regardless of the types of foveogenic forces acting there. Conversely, the evidence suggests that a predominance of midget pathways is necessary to generate the foveal morphology commonly seen in the Haplorrhine primates, including humans.

A diagrammatic representation of four stages in the development of the primate *fovea* is shown in Figure 6. The drawings depict midget-like circuits, involving a cone photoreceptor (red), a bipolar cell (blue) and a ganglion cell. A few rods are also shown (grey) and a notional amacrine cell type (pink); RPE cells are shown in dark blue. The approximate age represented by each image is indicated. The large gray arrows indicate the direction of the forces active at each stage.

Before the fovea forms (Fig 6A) retinal cells tend to be displaced *en masse* towards the incipient *fovea*. This effect has previously been referred to as *centripetal displacement*, and affects all cell layers, resulting in the central retina being very thick prior to formation of the *fovea*. The depression begins to form in the avascular zone, probably as a result of IOP acting perpendicular to the retinal plane (vertical arrow, Fig 6B), while the centripetal displacement of photoreceptors continues in the outer retina (large arrows). From around the time of birth (Fig 6C) ganglion cells as well as bipolar and amacrine cells, are displaced

away from the central *fovea* - so-called *centrifugal displacement*; this is indicated by the large arrows in the central inner retina. At birth there is a clear delay in the morphological development of the *fovea* cones; their inner and outer segments are much shorter than those on the foveal rim, and their axonal processes are just beginning to elongate. On the foveal rim, cone cell bodies have begun to stack so that there are now 2–3 layers of cells where they previously formed a monolayer.

The blood vessels that encircle the *fovea* develop anastomoses across the different layers at around birth, or just after. Within a few weeks (Fig 6D) excavation of the *fovea* has progressed so that there are relatively few ganglion or bipolar cells remaining in the pit. The inner and outer segments of the foveal cones have elongated so that they are longer than those on the rim; the cell bodies of the foveal cones are beginning to stack, and the pedicles of the cones are displaced out of the *fovea*. The changes that occur before the *fovea* is mature (see Fig 5D) include further elongation of the foveal cones, and more stacking of cell bodies - to achieve maximum packing density; further elongation of the axonal processes of foveal cones; displacement of pedicles, bipolar cells and ganglion cells out of the *fovea*, so that the cone cell bodies line the floor of the *fovea*, which in the adult is virtually devoid of other cell types. The fovea will also become shallower, and the foveal slope more gradual, as the retina is stretched by ocular growth.

4 Lessons From *In Vivo* Imaging

4.1 Introduction to *in vivo* imaging

Much of what we know about foveal anatomy derives from histological analysis of images like those shown in Fig 5. This approach has provided snapshot views of the developing macula and cellular structure of adult morphology. However, such an approach can only provide data about foveal morphology at a single time point, and in only a single plane of section. Recent years have seen the emergence of advanced imaging technologies that enable *in vivo* evaluation of the living retina. The ability to non-invasively assess foveal morphology, the avascular area, and photoreceptor density permits longitudinal studies in large populations. This new era of research in retinal structure and function promises to provide valuable insight into this important retinal area.

Optical coherence tomography (OCT) systems are based on interferometry, where light is sent through a sample arm and a reference arm and backscattered light from the sample is combined with that from the reference arm to generate an interference signal (Huang et al., 1991). The depth information of the reflected source is frequency encoded, with deeper reflections occurring at higher frequency. OCT provides images of the retinal layers, but current clinical devices lack cellular resolution due to the imperfect optics of the eye. Adaptive optics (AO) can be added to an imaging system to overcome the optical imperfection (aberrations) of the eye. AO systems have been incorporated into several imaging modalities, including fundus cameras, laser scanning ophthalmoscopes and OCT systems (Miller et al., 1996; Roorda et al., 2002; Zhang et al., 2005). The function of an AO system is to measure and correct aberrations of the human eye, to provide near diffraction-limited imaging. Several groups have now shown that it is possible to image both rod and cone photoreceptors, including foveal cones, the smallest photoreceptor cells in the retina (Dubra et al., 2011; Merino et al., 2011; Rossi et al., 2011). Much work has also been done to characterize the normal cone photoreceptor mosaic (Chui et al., 2008; Li et al., 2010; Song et al., 2011). In addition, many groups have developed motion-based techniques to examine the retinal vasculature, which makes it possible to noninvasively measure blood velocity and visualize the smallest foveal capillaries (Burns et al., 2008; Tam et al., 2010; Tam and Roorda, 2011).

Imaging devices that combine AO and OCT provides facility for studying the human retina *in vivo*, with resolution now beginning to approach that of histological methods. Several studies validating new imaging methods with histology have also been done (Brown et al., 2009; Drexler et al., 1999; Huang et al., 1991). These studies provide insight into the anatomical correlates of features visible on *in vivo* images (Figure 7). While most retinal layer correlates are well established (Catier et al., 2005), new debate has arisen on the precise correlates of the photoreceptor layer features in OCT images (Curcio et al., 2011; Spaide and Curcio, 2011). With the advent of these new technologies, there is a resurgence of interest in the anatomy and development of the *fovea*, providing the opportunity to study development of the *fovea* longitudinally, and to investigate in more detail the effects of premature birth and retinopathy of prematurity on foveal development (Dubis et al., 2012a; Maldonado et al., 2011; Vajzovic et al., 2012; Yanni et al., 2012).

4.2 Normal variation in foveal morphology - OCT

Many histological studies of the human *fovea* have been conducted over the last century, and more (Bach and Seefelder, 1914; Chievitz, 1888; Hendrickson and Yuodelis, 1984; Magitot, 1910; Mann, 1928; Polyak, 1941; Yamada, 1969). However, amongst these there is little if any, reference to individual variation in morphology, likely due to the relatively small number of retinas that have been examined. Non-invasive OCT imaging, has recently enabled an overview of foveal morphology in much larger sample, including normal and diseased eyes, revealing much greater diversity in morphology than previously anticipated (Dubis et al., 2012b; Dubis et al., 2009; Hammer et al., 2008; Tick et al., 2011; Wagner-Schuman et al., 2011).

One factor that has hampered comparison of findings from different teams has been a lack of consensus on the terms and methods used to define the different features of foveal morphology. These include **pit *depth*** - typically defined as the distance from the base of the *fovea* to a plane connecting the overlying foveal rim, or from the base to the level at which the *fovea* reaches a lateral radius of 728 μm; ***width / diameter*** - defined as either the subjective or objective rim-to-rim diameter or width of the region where nerve fiber layer is absent; ***slope*** - defined as either the *average* or *maximum* slope between the foveal center and the rim; and foveal *inner retinal area* - the cross-sectional area of the inner retinal tissue within 500μm of the foveal center, bordered by the *fovea*, the internal limiting membrane, and the outer plexiform layer (Dubis et al., 2012b; Dubis et al., 2009; Hammer et al., 2008; Kirby et al., 2009; Nolan et al., 2008; Tick et al., 2011). Other groups have investigated the *reflex pattern* caused by the pit (Delori et al., 2006) and *peak ganglion cell area* (Knighton et al., 2012). There has been a move towards unifying terminology, including the use of foveal *volume* as a measure of overall size (Dubis et al., 2012b). This measure has the advantage of capturing multiple aspects of foveal morphology, including depth and diameter. In the face of the varied metrics to describe the *fovea*, there remains a need for convergence on some objective measurements of *fovea* morphology, particularly for the purposes of comparing findings and developing measures that can be applied reliably in a clinical setting.

Despite these practical issues, diversity in foveal morphology has been identified in a number of studies. Hammer et al. (2008) examined five normal controls and found a mean (± SE) *fovea* depth of 121 ± 4.3 μm. They defined pit depth as the distance from the base of the pit to an arbitrarily chosen point where the pit reached a radius of 728 μm. Chui et al. (2009) used Spectralis spectral domain OCT to image eight normal emmetropic eyes and fit an 8^{th} order polynomial equation to the foveal contour to extract foveal depth, reporting a mean (± SD) pit depth of 137.56 ± 15.53 μm. One of the largest published collections of foveal metrics is derived from 180 subjects (Dubis et al., 2012b; Dubis et al., 2009; Wagner-Schuman et al., 2011) and show significant variation in foveal morphology in a normal

population, finding rim-to-rim diameter to vary by a factor >2 (1.12 – 2.57 mm), and depth to vary by a factor of at least 5.5 (0.032 – 0.176 mm).

Several groups have investigated race and gender as variables that affect foveal morphology. With respect to gender, Delori et al. (2006) used fundus reflectometry to estimate the diameter of the foveal depression in 18 subjects, finding that women had a significantly larger radius of foveal reflex than men (0.27 ± 0.07° *vs* 0.16 ± 0.04°, respectively). The authors interpreted this to mean that females have a "flatter foveal floor and/or broader foveal depression" (Delori et al., 2006; p529). This finding, however, conflicts with other reports (Kirby et al., 2009; Wagner-Schuman et al., 2011). A difficulty with using the foveal reflex as a parameter is that it is confounded by differences in axial length. Although a correction for refractive error was applied, on average men have longer axial lengths than women (Fotedar et al., 2010; Miglior et al., 1994), which can result in an underestimate of the radius of curvature of the ILM surface in men, compared to women. Nolan et al. (2008) used time domain OCT to examine foveal width, and found no significant gender difference in a sample of 59 subjects. Of the two approaches, one showed females to have slightly larger foveal diameters (Delori, 2006) while the other showed males to have larger diameters (Kirby et al., 2009). Another study (Wagner-Schuman et al., 2011) based on 90 subjects, including 43 females, in which differences in retinal magnification were accounted for, found no difference in foveal depth or diameter between the sexes.

In contrast, race is consistently and significantly correlated with differences foveal morphology (Nolan et al., 2008; Wagner-Schuman et al., 2011). Comparison of Caucasian and African/African American groups shows significant differences in pit depth, and diameter (Wagner-Schuman et al., 2011) such that Africans and African Americans are found to have significantly wider and deeper foveae than Caucasians (Figure 8 A–F). Consistent with this, another study finds white subjects to have significantly narrower foveal width measurements than non-white subjects (Nolan et al., 2008), although the magnitude of the difference reported is less than that reported by Wagner-Schuman et al (2011). A likely explanation for the discrepancy is the mixed composition of the `non-white' group which includes 5 Indian (who are in most contexts considered Caucasian), 6 Asian, 3 Hispanic/Spanish, and 4 Blacks, combined with the fact that individual differences in axial length were not taken into account (Nolan et al., 2008). This omission can result in mis-estimations of foveal diameter of up to 13% regardless of the method used to measure foveal diameter. Despite these issues, both studies indicate there is a genetic component that impacts foveal morphology. The developmental mechanism/s responsible for this and the implications for disease continue to be of interest.

4.3 Absence of the *fovea*: Relationship to the FAZ

Absence of a *fovea* (*foveal hypoplasia*) occurs in a number of conditions including congential nystagmus, in association with some Pax6 mutations, and with albinism (Azuma et al., 1996; Kinnear et al., 1985; Oetting et al., 1994; Oliver et al., 1987; Sonoda et al., 2000). The morphology of the FAZ is more difficult to detect by opthalmoscopy, but has been investigated using techniques such as entoptic viewing (Bradley et al., 1992; Levi et al., 1987; Zeffren et al., 1990) and fluorescein angiography (Zheng et al., 2010), as well as high-resolution imaging tools like OCT (Kim et al., 2011; Wang et al., 2011), AOSLO (Tam et al., 2010), and flood-illuminated AO ophthalmoscopy (Popovic et al., 2011). Collectively these studies show that the size of the FAZ is highly variable. Correlations of FAZ and foveal morphology also include findings indicating that patients with a history of retinopathy of prematurity have a small or absent FAZ (Mintz-Hittner et al., 1999) and modified foveal architecture, including increased retinal thickness within the fovea (Hammer et al., 2008; Wang et al., 2011; Yanni et al., 2012). Furthermore, two studies now show significant positive correlation between FAZ diameter and foveal size / volume (Dubis

et al., 2012b; Tick et al., 2011) adding weight to the hypothesis that FAZ and foveal morphology are closely linked, as described above (**2.3 and 2.4**).

The best studied of these groups are those with oculocutaneous albinism (OCA) and ocular albinism (OA) - who appear to lack an FAZ and have foveal hypoplasia (Marmor et al., 2008; McAllister et al., 2010; Seo et al., 2007) (Fig 8,G–I; Fig 9). OCA is further associated with retinal anomalies and visual deficits including loss of an annular reflex (Lee et al., 2001) and reduced visual acuity. The anomalies of visual function have been attributed to a number of factors, including wiring errors in the brain (Kaas, 2005; Schmolesky et al., 2000), absence of melanin synthesis and maldevelopment of the *fovea*, *per se* (Seo et al., 2007).

The associations are not clear-cut, however. For example, some individuals with residual enzyme activity and some melanin pigment in the macula have decreased visual acuity, while others with poorly defined foveas have relatively normal visual acuity (Harvey et al., 2006; Summers, 1996). Furthermore, prior to the application of OCT to the question, both histological and physiological studies arrived at a range of different, often conflicting conclusions, regarding the impact of albinism on the macula, in particular the cone mosaic. For example, Fulton et al. (1978) found by histology that central cone density in a patient with OCA was significantly *decreased* compared to values normally found in the parafoveal region, while another histological study detected *increased* cone density in the *fovea* area compared with the periphery (Akeo et al., 1996). Wilson et al. (1988) measured grating acuity in two OCA patients and found a defect in spatial processing in the central retina that was best explained by an *increased* spacing of the central cone photoreceptors while multifocal electroretinogram findings have inferred that the density of cone photoreceptors across the central retina is uniform in OCA (Kelly and Weiss, 2006) and also in ocular albinism (OA) (Nusinowitz and Sarraf, 2008).

The broad spectrum of phenotypes associated with foveal hypoplasia, including the wide range of albinotic phenotypes, is a valuable experimental group which can be used to evaluate the relationship of the FAZ with (i) morphology of the *fovea*, (ii) packing of cones in the central cone mosaic, and (iii) visual function. An investigation of 4 individuals (2 albinotic, and 2 normally pigmented) lacking a *fovea*, carried out by Marmor et al (2008) found absent FAZ, combined with normal multifocal ERG responses, acuities in the low end of the normal range, thickening of the central ONL associated with lengthening of inner an outer segments by OCT, and normal cone diameters in the central 1–2 degrees of retina (by adaptive optics). Although based on a small sample, the findings suggested that absence of a *fovea* does not necessarily have a major impact on visual function. A second study (McAllister et al., 2010) also used AO devices and commercial OCT systems to evaluate four individuals with OCA1B and two with OA1. The findings show varying degrees of cone specialization and `foveal' morphologies – ranging from presence of a dome, through to shallow pits - supporting the idea that normal foveal development is `arrested' in individuals with albinism (Wilson et al., 1988) and that significant central cone specialization can occur in the absence of a *fovea* (Fig 9). It has also been noted that in anencephaly, foveal cone specialization (cone packing and elongation) occurs in the absence of a fully formed *fovea* (Hendrickson et al., 2006a). The data indicate that the factors which mediate cone specialization in central retina are complex, and do not support the passive / mechanical model proposed by Springer (1999).

4.4 The FAZ, photoreceptor density and the fixation point

It is widely accepted that during fixation foveal photoreceptors are oriented towards the object of interest (Barlow, 1952; Walls, 1937; Weymouth et al., 1928). Relatively few studies, however, have attempted to identify where the fixation point falls within the foveal

photoreceptor mosaic (Bradley et al., 1992; Putnam et al., 2005; Rossi and Roorda, 2010; Zeffren et al., 1990). Entopic viewing has been used by both Zeffren and colleagues (1990) and Bradley and colleagues (1992) to map the FAZ in 26 eyes (14 subjects), finding that on average, the retinal point of fixation is 65±50 μm (±SD) from the geographic center of the FAZ. They found no correlation between this value and size of the FAZ. More recently, AO has been applied to this question (Putnam et al., 2005). These investigators directly imaged the central foveal cone photoreceptor mosaic in 5 subjects with stable fixation (±17 μm) using AO, and a CCD camera aligned such that the center of the fixation target fell at the center of a 512 × 512 CCD array. Using this approach the authors were able to show that the region of peak cone density in the foveal cone mosaic is not always used for fixation. These studies indicate that the locus of fixation is on average 50 μm from the locus of peak cone density. Further studies are required to establish the locus of the peak cone density in relation to the geometrical centre of the FAZ.

4.5 Development of the *fovea* - OCT

Maturation of the *fovea* and central photoreceptors in non-anesthetized premature infants has recently become the subject of a number of *in vivo* studies, using hand-held spectral domain OCT devices (Dubis et al., 2012a; Maldonado et al., 2011; Vajzovic et al., 2012). Because the *fovea* begins to emerge between 25 and 27 WG, a significant number of premature infants that survive very early birth will have foveas that develop entirely in the *ex utero* environment. The findings from these studies show that foveal development *ex utero* is comparable with *in utero* development, based on histological findings (Maldonado et al., 2011; Vajzovic et al., 2012), and that the range of foveal morphologies detected in adult retinas appears to be evident in the individual differences in foveal morphology apparent early in development (Dubis et al., 2012a). Histological studies also suggested that foveal cones may take up to several years to reach adult proportions (Hendrickson and Yuodelis, 1984; Yuodelis and Hendrickson, 1986) although the OCT studies now indicate that maturation of foveal cones occurs over a period as short at 18 months (Dubis et al., 2012a; Maldonado et al., 2011).

The use of OCT to track development of the *fovea* has highlighted an observation initially made around 100 years ago, featured in the drawings of developing retina published by Bach and Seefelder (1914) and re-published in the seminal work on development of the human eye by Ida Mann (1928). That is, that the cones that line the developing *fovea* are the very last to elongate and obtain adult-like morphology (see above, **3.3**). Thus in OCT images of preterm retinas and newborn retinas only a single hyper-reflective band can be seen in outer retina, whereas in adult retinas 4 hyper-reflective bands are present (Maldonado et al., 2011). Comparison of histological images with OCT images at selected developmental timepoints has shown that emergence of the multiple bands in outer retina is closely correlated with morphological development of photoreceptors, and particularly the elongation of the inner and outer segments of the foveal cones. (Dubis et al., 2012a; Hendrickson et al., 2012; Vajzovic et al., 2012).

5. Adaptive Advantages of a *Fovea*?

What then is the optical value of the *fovea*? The conventional wisdom is that the inner retinal elements, that might blur or scatter light, including cells and their processes, are swept aside for the sake of high acuity vision. Psychophysical data show that only within the central *fovea* is resolution limited by cone spacing; immediately outside the foveal centre resolution is better matched to the sampling limits of Midget ganglion cells (Rossi and Roorda, 2010). However, surprisingly little hard evidence has been presented to demonstrate why this is the case.

Both the nerve fibre layer (NFL) and the Henle layer are made up of bundles of axonal processes which on OCT are highly scattering; this scattering should be worse at visible wavelengths, compared to the long wavelengths used for OCT imaging. So one optical advantage of the fibre arrangements seen at the *fovea* is that the radiating pattern of axon bundles in the NFL surrounding the *fovea*, and the thinner Henle fibre in central *fovea* (*cf.* parafovea), is in the reduced light scatter. However, the profile of the pit seems to have little obvious optical benefit (Williams, 1980), and as discussed above (**2.3** and **4.3**) visual acuity in *Foveal hypoplasia* is in the normal range, for some individuals. What role/s then does the pit play in enhancing resolution at the *fovea*, if any?

5.1 Photoreceptors act as waveguides

A striking feature of a *fovea* is the narrowing and elongation of the central-most inner and outer segments, which allows for their packing at high spatial density. The *high density* is important for improving the spatial sampling in the central photoreceptor array. Their narrow diameter, combined with particular physical properties (having a dense core surrounded by less dense material) means that they will operate as highly effective waveguides for visible light (Snyder, 1975; Stavenga, 2003) (Enoch, 1980). Why the foveal photoreceptors are *more elongated* than those throughout the macula, for example, is likely due to the fact that if a narrow photoreceptor is to absorb the same amount of light as a neighbor that is thicker, it will be necessarily be longer so that it can accommodate a similar volume of opsin.

Given perfect optics, the angular resolution of an eye is proportional to the diameter of the pupil, relative to the wavelength of the light, λ/D (Snyder, 1975). The angular diameter of the photoreceptors should match that angle in order to use of the resolution made available by the pupil. In a high-resolution eye this implies very small photoreceptor diameters - but there are limits.

The family of modes supported by a waveguide, and the relative power in each, is determined by the dimensionless wave guide parameter `V', where $V = (\pi d/\lambda)\times(n_i^2 - n_o^2)^{0.5}$; n_i and n_o are the refractive indices of the inside of the guide (core) and the outside (cladding) respectively; d is the diameter of the core - in this case, the internal diameter of the inner and outer segments of photoreceptors (Snyder, 1975). Below V=2.3 only the lowest order mode is supported, providing a so-called *mono-modal* optical fibre, which absorbs light very directionally. However, when d falls to a critical low value (where$1<V<2$) the amount of light inside the guide will rapidly drop to zero, and be propagated outside the core - an undesirable outcome that sacrifices focus. Above V=2.3 the receptors are progressively less directional. Because of these effects, cone photoreceptors sensitive to visible wavelengths should be no less than ~2 μm in diameter. A consequence is that to achieve diffraction-limited resolution, eyes with large pupils (and good optics) need to grow in diameter to match the smallest possible photoreceptor to the angular resolution provided by larger pupils; this has consequences.

Using a digital camera as an analogy, for a *fovea* of ~1 mm diameter, comprising 2 μm cone segments, the resultant `camera' comprises only about 227K hexagonally packed pixels (cones); this is equivalent to a low-grade digital camera with a resolving power of only 0.25 mega-pixels. Of course, the visual system deals with this sampling problem using other strategies. However, that there is such a coarse sampling system in the human retina implies that there is a physiological limit on its diameter, otherwise why not evolve a larger `camera' with more `pixels'? Indeed, a study of foveal dimensions in 5 New World monkeys, a rhesus monkey and a human finds that although retinal area varies overall by a factor of 5, the area of the *fovea* is approximately the same size in all species, supporting the idea that the size of the *fovea* is physiologically constrained (Franco et al., 2000). Furthermore, we now

understand from OCT studies that narrowing and elongation of cones can occur in the absence of a *fovea* (see **4.2),** leading to the question, *why have a fovea at all?*

5.2 The Stiles-Crawford effect

Roorda (2002) has shown that foveal cones are sufficiently crystalline to have the acceptance angle of a single monomodal photoreceptor. This results in the Stiles-Crawford effects (SC), where collimated pencils of light entering the pupil parallel to, but offset from, the optical axis of the eye appear dimmer than those on the optical axis (Figure 10). Effectively this means that the pupil is apodized (Atchison et al., 2003; Atchison et al., 2002); that is, the pupil acts like a neutral density filter which increases in density, radially and outwards. The SC apodization is roughly Gaussian in shape, but the part imposed on the pupil is less than ±1 SD (Rynders et al., 1995; Schulze-Dobold et al., 2009), and so does not reduce the effective diameter of the pupil greatly. Nonetheless, the consequence of having a crystalline array of waveguiding cones in our *fovea* is that the effective pupil size for optimal central vision is smaller than for the rest of the retina. Importantly, apodization ameliorates optical aberrations.

Overall, the effect is that for pupil diameters >2.5 mm, the *fovea* receives less light but sees fewer aberrations than extrafoveal retina; in contrast, the retina outside the *fovea* benefits from higher signal-to-noise ratios due to a denser rain of photons. For Poisson processes like photon arrivals, signal-to-noise ratios scale with the square root of the number of absorptions per second. Information (bits / sec) scales linearly with the number of samples (cones), but with the log of the signal-to-noise ratio (Snyder et al., 1977). Thus in information terms, a small relative loss of foveal photons caused by apodizing, can be more than made up for by increasing the number of independent samples provided by higher cone densities and a well-focussed image.

The SC effect on letter acuity have been illustrated by Atchison et al. (2002)[d] (Fig 10) which shows the effects of doubling or removing the SC apodization. Although difficult to quantify, the subjective improvement of image quality provided by the SC effect seems obvious enough. However, given that this effect is due to the narrowness of cones, and we know that cones can be elongated and narrow in the absence of a *fovea*, what does this tell us about the adaptive advantage of the *fovea, per se?*

5.3 Müller cell processes as waveguides?

Recent evidence suggests that waveguides are also components of vertebrate eyes in the absence of a *fovea*. That is, Müller glial cells can also act as optical waveguides, potentially providing a fibre optic *transfer plate* between inner and outer retina (Agte et al., 2011; Franze et al., 2007; Labin and Ribak, 2010). Coherent optical fibre bundles are an extreme example of a transfer plate: ideally the image at one end of the coherent bundle is transferred unchanged to the other end. The Müller cells are often called *radial* glia because they span the retina from the inner limiting membrane to the external limiting membrane. Their filaments are about the right diameter to act as multimodal light guides (V>2.3). Figure 11 shows guinea pig Müller cells guiding two narrow laser beams through the retina producing two reasonably resolved blobs of light at the photoreceptor layer (Agte et al., 2011). The spreading of the light indicates that, although effective, the transfer plate effect is imperfect. However, it shows the upper limit of how good the image quality might be when light is conducted by Müller cell processes.

In the *fovea*, however, Müller cell processes run parallel to the Henle fibres (Distler and Dreher, 1996; Yamada, 1969), which cross the retina diagonal to the incoming light. They are not smooth, but include abrupt kinks, or bends, along their length (Reichenbach and

Bringmann, 2010). Thus, Müller Cells cannot act as a transfer plate in the central *fovea* because of their oblique orientation to light, and their uneven profile.

So a possible adaptive advantage of a *fovea* is that it *prevents* Müller cells from acting as a bad transfer plate, instead allowing the crystalline lattice of foveal photoreceptors to act as a near-perfect one. It is possible to reason how this might evolve. That is, as pupil and eye size increased in the quest for better acuity, the diameter of the cone outer segments would also decrease to their minimum, and their length increase to the amount required, predisposing them to form a crystalline lattice. Then, if there were a developmental `accident' that reduced the adverse side-effects of Müller cell waveguides, i.e. pushing the inner retina and the Müller cells aside, the benefits of the cone-mediated Stiles-Crawford effect would be automatic, and so perhaps highly selected for.

5.4 Fresnel numbers and the *fovea*

Fresnel numbers describe the diffraction effects of electromagnetic radiation passing through an aperture, and can be applied to an understanding how the different wavelengths of radiation that pass through the pupil are dispersed in the eye. The Fresnel number is described by the equation $N = a^2/(\lambda f)$, where f is the focal length, and a is the pupil radius. In most camera systems N is large and the distribution of light on either side of the focal point of the lens is symmetrical. However, when N is small the distribution of light on either side of the focus becomes asymmetrical. In particular, the peak of the axial intensity moves closer to the lens than is predicted by geometric optics (Holmes et al., 1972; Li and Wolf, 1981; Stavenga, 2003). At visible wavelengths N for the human eye is large, but that is not true in the infrared range.

For wavelengths > 1.2 μm infrared transmission of the eye is similar to that of water, and in general transmission drops rapidly with increasing wavelength. However, there are relative *windows* that allow increased transmission of wavelengths of 1.25, 1.7 2.2 and 3.70 μm, where transmission is increased by 10 to 100 times (although it is still 10 to 100 times less than for visible wavelengths). Therefore it is possible that bright sunlight may cause significant fluence (J/cm^2) in the eye at these wavelengths, and generate heat in regions where these wavelengths are in, or near focus. Recently, work has shown that lipid-rich tissues are hundreds of times more absorbing of wavelengths of 3.80 μm than other cellular media, to the point where radiation of this wavelength has been suggested as a plausible way to ablate atherosclerotic plaques, without damaging artery tissue (Ke et al., 2009). Thus, such radiation propagated in the eye could be problematic for the axon-rich layers which contain high levels of lipid (Nag et al., 2011) and are abundant in the Henle fibre layer and on the surface of the retina.

Figure 12 shows the shift of the focal point towards the lens (away from the *fovea*) at different wavelengths for 3 pupil diameters, and indicates positions of the infrared `windows'. The shifts of the focal point described by the Fresnel numbers are equivalent to as much as 80μm - 50% mean macular thickness (Wexler et al., 2010), or almost the depth of the pit (Dubis et al., 2009). Thus, for visible light focused on the retinal/vitreal border, the focal point for 2000 to 4000 nm light would be located in the vitreous at about the level of the foveal rim, affording protection to the lipid-rich Henle Fibres from the effects of infra-red radiation. Although the solar irradiance at these wavelengths is 10 to 30 times less than for visible light, when looking at highly specular reflections or the sun, the risk of damage may still be significant.

5.5 What *are* the optical advantages of a *fovea*?

The available data appears to suggest that foveal architecture *per se* is not strictly correlated with acuity. A small study by Marmor (2008) shows that individuals lacking a fovea have acuity in the normal range towards the low end, while studies of foveal morphology in individuals born prematurely show that foveal structure is modified by premature birth, but that there is no clear correlation between foveal morphology and acuity (Akerblom et al., 2011; Hammer et al., 2008) (Wang et al., 2012; Yanni et al., 2012). A weakness in those findings is that none have made corrections for variations in foveal architecture that are genetically based (Nolan et al., 2008; Wagner-Schuman et al., 2011, and to our knowledge there has been no systematic study that attempts to correlate acuity with foveal architecture as a primary variable.

Setting aside the advantage of excluding blood vessels from the optic axis, overall the optical advantages of the foveal pit itself appear to be relatively minor. These include deriving benefit from the Stiles-Crawford effects by wave-guiding, and by removing the possibility that poorly constructed Muller cell transfer plates might degrade image quality. OCT informs us that photoreceptors in the macular region are significantly elongated even when the *fovea* is absent. However, as far as we know, when the fovea is absent there is no point where there is a focal concentration of slightly narrower and more elongated cones, as is seen in a *foveola*. Data from macaque monkeys suggests that cones in the *foveola* are approximately half the diameter of those on the edge (Borwein et al., 1980). The extent to which this grading of cone inner segment diameters / cone apertures within a *fovea* contributes favorably to resolving power, perhaps by deriving additional benefit from the SC effect, is difficult to evaluate.

The presence of a *fovea* may also protect axons of foveal cones from being `cooked' by infrared radiation reaching the retinal surface as a result of transmission `windows' in ocular tissues and media. It is interesting that these putative advantages derive ultimately from the wavelengths of light that enter the eye, in that the minimum diameter of photoreceptor inner and outer segments is determined by wavelength, and limits the number of cones within the foveal cone mosaic. The resultant rather coarse sampling array of cones at the *fovea* suggests that, for other biological reasons, the FAZ and hence the *fovea* cannot evolve to a larger size.

6. Overview and Future Directions

This review addresses recent advances in understanding the adaptations of central primate retina associated with high acuity vision. Findings suggest that of primary importance is vascular specialization that obviates the possibility of angioscotomas formed by the shadows of vessels falling onto a cone-rich mosaic. Hence, microvessels dominate the *areae centrales* of afoveate retinas, and the central area of foveate species in which definition of an FAZ is prerequisite for formation of a fovea.

In central retina a distinct set of molecular factors control vascular patterning, and anti-angiogenic PEDF appears to define the FAZ. It also appears that the axon guidance factor EphA6, has a dual role in mapping ganglion cell axons onto targets in the brain, and in regulating the migration of astrocytes across the retina, influencing the patterning of vessels and affecting their slow rate of growth towards the developing macula. Variations in the spatiotemporal expression of these, and other yet unidentified factors, is likely to explain the diversity in foveal architecture that is recognized both on genetic bases (*e.g.* albinism and race) and in response to environmental influences (*e.g.* prematurity).

The relationship between foveal morphology (including the condition of *hypoplasia*), cone diameter, packing density, the fixation point, and visual acuity is a new area of investigation now available using *in vivo* techniques. Such studies will better inform our understanding of the factors that determine acuity functions, and clarify the different roles played by the shape of the *fovea* and by cone density. Our present analysis suggests that any optical advantage derived *per se* from the presence of a *fovea,* results from the cumulative effect of a number of variables, and that no single factor, as far as we can presently determine, has a major impact on visual resolution at the *fovea*.

A crucial factor affecting visual acuity is the high density of cones in the foveal cone mosaic, and the midget circuits that dominate central, cell-rich retina which is thickest on the margins of the *fovea* (Provis et al., 2005), creating a local micro-environment where oxygen is in high demand (Yu et al., 2005). Thus, we have evolved a central retina that relies on a high concentration of cells – required to improve bandwidth for signals from central retina – hand in hand with mechanisms that constrain retinal blood supply, to the extent that the macular region is heavily reliant on an extensive network of microvessels both within the retina, and in the form of the choriocapillaris.

It seems likely that vulnerability to macular degeneration is significantly affected by this arrangement (Provis et al., 2005), particularly in the presence of other genetic and environmental predisposing factors (Sparrow et al., 2012). Microvessels are vulnerable to a variety of stressors, and dysfunction is associated with risk factors in common with macular degeneration, including smoking (Harris et al., 2012), and with a wide range of CNS pathologies (Grammas et al., 2011). Because microvessels feature so prominently in the normal anatomy and physiology of the macula, it seems likely that susceptibility to AMD is closely linked with incipient microvascular disease.

Acknowledgments

The authors are grateful to all participants in the research that has informed this article, including tissue donors and scan subjects. TM and JP are supported by the Australian Research Council Centre of Excellence (CE0561903). AD was supported by the NIH (T32 EY014537). JC acknowledges support from the NIH (P30 EY001931, R01 EY017607, C06 RR016511), Research to Prevent Blindness and the Foundation Fighting Blindness.

Abbreviations

AO	Adaptive optics
dLGN	dorsal lateral geniculate nucleus
dPC	days post-conception
FAZ	foveal avascular zone
GCL	ganglion cell layer
INL	inner nuclear layer
OA	ocular albinism
OCA	oculo-cutaneous albinism
OCT	optical coherence tomography
ONL	outer nuclear layer
SCE	Stiles-Crawford Effects

References

Abramov I, Gordon J, Hendrickson A, Hainline L, Dobson V, LaBossiere E. The retina of the newborn human infant. Science. 1982; 217:265–7. [PubMed: 6178160]

Adams DL, Horton JC. The representation of retinal blood vessels in primate striate cortex. J Neurosci. 2003; 23:5984–97. [PubMed: 12853416]

Agte S, Junek S, Matthias S, Ulbricht E, Erdmann I, Wurm A, Schild D, Kas JA, Reichenbach A. Muller glial cell-provided cellular light guidance through the vital guinea-pig retina. Biophysical journal. 2011; 101:2611–9. [PubMed: 22261048]

Akeo K, Shirai S, Okisaka S, Shimizu H, Miyata H, Kikuchi A, Nishikawa T, Suzumori K, Fujiwara T, Majima A. Histology of fetal eyes with oculocutaneous albinism. Arch Ophthalmol. 1996; 114:613–6. [PubMed: 8619776]

Akerblom H, Larsson E, Eriksson U, Holmstrom G. Central macular thickness is correlated with gestational age at birth in prematurely born children. Br J Ophthalmol. 2011; 95:799–803. [PubMed: 20974631]

Atchison DA, Marcos S, Scott DH. The influence of the Stiles-Crawford peak location on visual performance. Vision Res. 2003; 43:659–68. [PubMed: 12604102]

Atchison DA, Scott DH, Strang NC, Artal P. Influence of Stiles-Crawford apodization on visual acuity. J Opt Soc Am A Opt Image Sci Vis. 2002; 19:1073–83. [PubMed: 12049344]

Azuma N, Nishina S, Yanagisawa H, Okuyama T, Yamada M. PAX6 missense mutation in isolated foveal hypoplasia. Nat Genet. 1996; 13:141–2. [PubMed: 8640214]

Bach, L.; Seefelder, R. Entwicklungsgeschichte des menschlichen auges. W. Engelmann Leipzig. 1914.

Barlow HB. Eye movements during fixation. J Physiol. 1952; 116:290–306. [PubMed: 14939180]

Becerra P, Fariss RN, Wu YQ, Montuenga LM, Wong P, Pfeffer BA. Pigment epithelium-derived factor in the monkey retinal pigment epithelium and interphotoreceptor matrix: apical secretion and distribution. Experimental Eye Research. 2004; 78:223–34. [PubMed: 14729355]

Bernstein SL, Borst DE, Neuder ME, Wong P. Characterization of a human fovea cDNA library and regional differential gene expression in the human retina. Genomics. 1996; 32:301–8. [PubMed: 8838792]

Bernstein SL, Borst DE, Wong PW. Isolation of differentially expressed human fovea genes: candidates for macular disease. Mol Vis. 1995; 1:4. [PubMed: 9238082]

Bhutto IA, McLeod DS, Hasegawa T, Kim SY, Merges C, Tong P, Lutty GA. Pigment epithelium-derived factor (PEDF) and vascular endothelial growth factor (VEGF) in aged human choroid and eyes with age-related macular degeneration. Exp Eye Res. 2006; 82:99–110. [PubMed: 16019000]

Borwein B, Borwein D, Medeiros J, McGowan JW. The ultrastructure of monkey foveal photoreceptors, with special reference to the structure, shape, size, and spacing of the foveal cones. American Journal of Anatomy. 1980; 159:125–46. [PubMed: 7446444]

Bradley A, Applegate RA, Zeffren BS, van Heuven WA. Psychophysical measurement of the size and shape of the human foveal avascular zone. Ophthalmic Physiol Opt. 1992; 12:18–23. [PubMed: 1584610]

Brown NH, Koreishi AF, McCall M, Izatt JA, Rickman CB, Toth CA. Developing SDOCT to assess donor human eyes prior to tissue sectioning for research. Graefes Arch Clin Exp Ophthalmol. 2009; 247:1069–80. [PubMed: 19225801]

Bunt AH, Hendrickson AE, Lund JS, Lund RD, Fuchs AF. Monkey retinal ganglion cells: Morphometric analysis and tracing of axonal projections, with consideration of the peroxidase technique. Journal of Comparative Neurology. 1975; 164:265–86. [PubMed: 810500]

Burns SA, Zhangyi Z, Chui TYP, Song H, Elsner AE, Malinovsky VE. Imaging the Inner Retina Using Adaptive Optics. Investigative Ophthalmology & Visual Science. 2008; 49

Buttery RG, Haight JR, Bell K. Vascular and avascular retinae in mammals. A funduscopic and fluorescein angiographic study. Brain, Behavior & Evolution. 1990; 35:156–75.

Buttery RG, Hinrichsen CF, Weller WL, Haight JR. How thick should a retina be? A comparative study of mammalian species with and without intraretinal vasculature. Vision Research. 1991; 31:169–87. [PubMed: 2017880]

Catier A, Tadayoni R, Paques M, Erginay A, Haouchine B, Gaudric A, Massin P. Characterization of macular edema from various etiologies by optical coherence tomography. American journal of ophthalmology. 2005; 140:200–6. [PubMed: 15992752]

Chalupa L, Lia B. The nasotemporal division of retinal ganglion cells with crossed and uncrossed projections in the fetal Rhesus monkey. Journal of Neuroscience. 1991; 11:191–202. [PubMed: 1702463]

Chan-Ling T, Halasz P, Stone J. Development of retinal vasculature in the cat: processes and mechanisms. Current Eye Research. 1990; 9:459–78. [PubMed: 2166637]

Chase J. The evolution of retinal vascularization in mammals. Ophthalmology. 1982; 89:1518–25. [PubMed: 7162797]

Chievitz J. Entwicklund der fovea centralis retinae. Anat. Anzeig.Jena. Bd III S. 1888:579.

Chui TY, Song H, Burns SA. Individual variations in human cone photoreceptor packing density: variations with refractive error. Invest Ophthalmol Vis Sci. 2008; 49:4679–87. [PubMed: 18552378]

Cooper ER. The development of the human lateral geniculate body. Brain. 1945; 68:222–39. [PubMed: 21017988]

Cornish EE, Madigan MC, Natoli RC, Hales A, Hendrickson A, Provis JM. Gradients of cone differentiation and FGF expression during development of the foveal depression in macaque retina. Visual Neuroscience. 2005; 22:447–59. [PubMed: 16212702]

Cornish EE, Natoli RC, Hendrickson A, Provis JM. Differential distribution of fibroblast growth factor receptors (FGFRs) on foveal cones: FGFR-4 is an early marker of cone photoreceptors. Molecular Vision. 2004; 10:1–14. [PubMed: 14737068]

Curcio CA, Messinger JD, Sloan KR, Mitra A, McGwin G, Spaide RF. Human chorioretinal layer thicknesses measured in macula-wide, high-resolution histologic sections. Invest Ophthalmol Vis Sci. 2011; 52:3943–54. [PubMed: 21421869]

Delori FC, Goger DG, Keilhauer C, Salvetti P, Staurenghi G. Bimodal spatial distribution of macular pigment: evidence of a gender relationship. J Opt Soc Am A Opt Image Sci Vis. 2006; 23:521–38. [PubMed: 16539047]

Diaz-Araya C, Provis JM. Evidence of photoreceptor migration during early foveal development: a quantitative analysis of human fetal retinae. Vis Neurosci. 1992; 8:505–14. [PubMed: 1586652]

Distler C, Dreher Z. Glia cells of the monkey retina--II. Muller cells. Vision research. 1996; 36:2381–94. [PubMed: 8917802]

Dkhissi-Benyahya O, Szel A, Degrip WJ, Cooper HM. Short and mid-wavelength cone distribution in a nocturnal Strepsirrhine primate (Microcebus murinus). J Comp Neurol. 2001; 438:490–504. [PubMed: 11559903]

Drexler W, Morgner U, Kartner FX, Pitris C, Boppart SA, Li XD, Ippen EP, Fujimoto JG. In vivo ultrahigh-resolution optical coherence tomography. Opt Lett. 1999; 24:1221–3. [PubMed: 18073990]

Dubis AM, Costakos DM, Subramaniam CD, Godara P, Wirostko WJ, Carroll J, Provis JM. Examination of Normal Human Foveal Development Using Optical Coherence Tomography and Histology. Archives of Ophthalmology. 2012a; 130:1291–300. [PubMed: 23044942]

Dubis AM, Hansen BR, Cooper RF, Beringer J, Dubra A, Carroll J. Relationship between the foveal avascular zone and foveal pit morphology. Invest Ophthalmol Vis Sci. 2012b; 53:1628–36. [PubMed: 22323466]

Dubis AM, McAllister JT, Carroll J. Reconstructing foveal pit morphology from optical coherence tomography imaging. Br J Ophthalmol. 2009; 93:1223–7. [PubMed: 19474001]

Dubra A, Sulai Y, Norris JL, Cooper RF, Dubis AM, Williams DR, Carroll J. Noninvasive imaging of the human rod photoreceptor mosaic using a confocal adaptive optics scanning ophthalmoscope. Biomed Opt Express. 2011; 2:1864–76. [PubMed: 21750765]

Dyer MA, Martins R, da Silva Filho M, Muniz JA, Silveira LC, Cepko CL, Finlay BL. Developmental sources of conservation and variation in the evolution of the primate eye. Proc Natl Acad Sci U S A. 2009; 106:8963–8. [PubMed: 19451636]

Eglen SJ, Demas J, Wong RO. Mapping by waves. Patterned spontaneous activity regulates retinotopic map refinement. Neuron. 2003; 40:1053–5. [PubMed: 14687538]

Enoch JM. Vertebrate receptor optics and orientation. Doc Ophthalmol. 1980; 48:373–88. [PubMed: 6995055]

Fawzi AA, Lee N, Acton JH, Laine AF, Smith RT. Recovery of macular pigment spectrum in vivo using hyperspectral image analysis. Journal of Biomedical Optics. 2011; 16:106008. [PubMed: 22029355]

Fotedar R, Wang JJ, Burlutsky G, Morgan IG, Rose K, Wong TY, Mitchell P. Distribution of axial length and ocular biometry measured using partial coherence laser interferometry (IOL Master) in an older white population. Ophthalmology. 2010; 117:417–23. [PubMed: 20031227]

Franco EC, Finlay BL, Silveira LC, Yamada ES, Crowley JC. Conservation of absolute foveal area in New World monkeys. A constraint on eye size and conformation. Brain Behav Evol. 2000; 56:276–86. [PubMed: 11251320]

Franze, K.; Grosche, J.; Skatchkov, SN.; Schinkinger, S.; Foja, C.; Schild, D.; Uckermann, O.; Travis, K.; Reichenbach, A.; Guck, J. Muller cells are living optical fibers in the vertebrate retina; Proceedings of the National Academy of Sciences of the United States of America; 2007. p. 8287-92.

Fulton AB, Albert DM, Craft JL. Human albinism. Light and electron microscopy study. Arch Ophthalmol. 1978; 96:305–10. [PubMed: 629678]

Gilbert MS. The early development of the human diencephalon. The Journal of Comparative Neurology. 1935; 62:81–115.

Grammas P, Martinez J, Miller B. Cerebral microvascular endothelium and the pathogenesis of neurodegenerative diseases. Expert Rev Mol Med. 2011; 13:e19. [PubMed: 21676288]

Grünert U, Greferath U, Boycott BB, Wässle H. Parasol (Pa) ganglion cells of the primate fovea: Immunocytochemical staining with antibodies against $GABA_A$-receptors. Vision Research. 1993; 33:1–14. [PubMed: 8383899]

Hammer DX, Iftimia NV, Ferguson RD, Bigelow CE, Ustun TE, Barnaby AM, Fulton AB. Foveal fine structure in retinopathy of prematurity: an adaptive optics Fourier domain optical coherence tomography study. Invest Ophthalmol Vis Sci. 2008; 49:2061–70. [PubMed: 18223243]

Harris B, Klein R, Jerosch-Herold M, Hoffman EA, Ahmed FS, Jacobs DR Jr. Klein BEK, Wong TY, Lima JAC, Cotch MF, Barr RG. The association of systemic microvascular changes with lung function and lung density: a cross-sectional study. PloS one. 2012; 7:e50224. [PubMed: 23284634]

Harvey PS, King RA, Summers CG. Spectrum of foveal development in albinism detected with optical coherence tomography. J AAPOS. 2006; 10:237–42. [PubMed: 16814177]

Hendrickson A, Djajadi H, Erickson A, Possin D. Development of the human retina in the absence of ganglion cells. Exp Eye Res. 2006a; 83:920–31. [PubMed: 16793038]

Hendrickson A, Possin D, Vajzovic L, Toth CA. Histologic development of the human hovea From midgestation to maturity. Am J Ophthalmol. 2012; 154:767–78 e2. [PubMed: 22935600]

Hendrickson A, Troilo D, Possin D, Springer A. Development of the neural retina and its vasculature in the marmoset Callithrix jacchus. J Comp Neurol. 2006b; 497:270–86. [PubMed: 16705674]

Hendrickson AE, Yuodelis C. The morphological development of the human fovea. Ophthalmology. 1984; 91:603–12. [PubMed: 6462623]

Henkind P, Bellhorn RW, Murphy ME, Roa N. Development of macular vessels in monkey and cat. Br J Ophthalmol. 1975; 59:703–9. [PubMed: 814917]

Hevner RF. Development of connections in the human visual system during fetal midgestation: a DiI-tracing study. J Neuropathol Exp Neurol. 2000; 59:385–92. [PubMed: 10888368]

Holmes DA, Korka JE, Avizonis PV. Parametric study of apertured fucused Gaussian beams. Applied Optics. 1972; 11:565–74. [PubMed: 20111549]

Hornan DM, Peirson SN, Hardcastle AJ, Molday RS, Cheetham ME, Webster AR. Novel retinal and cone photoreceptor transcripts revealed by human macular expression profiling. Invest Ophthalmol Vis Sci. 2007; 48:5388–96. [PubMed: 18055785]

Horton JC, Adams DL. The cortical representation of shadows cast by retinal blood vessels. Trans Am Ophthalmol Soc. 2000; 98:33–8. discussion 38–9. [PubMed: 11190031]

Huang D, Swanson EA, Lin CP, Schuman JS, Stinson WG, Chang W, Hee MR, Flotte T, Gregory K, Puliafito CA, et al. Optical coherence tomography. Science. 1991; 254:1178–81. [PubMed: 1957169]

Huberman AD, Feller MB, Chapman B. Mechanisms underlying development of visual maps and receptive fields. Annual Review of Neuroscience. 2008; 31:479–509.

Huberman AD, Murray KD, Warland DK, Feldheim DA, Chapman B. Ephrin-As mediate targeting of eye-specific projections to the lateral geniculate nucleus. Nat Neurosci. 2005; 8:1013–21. [PubMed: 16025110]

Hughes A. Topographical relationships between the anatomy and physiology of the rabbit visual system. Documenta Ophthalmologica. 1971; 30:33–159. [PubMed: 5000058]

Hughes A. A quantitative analysis of the cat retinal ganglion cell topography. Journal of Comparative Neurology. 1975; 163:107–28. [PubMed: 1159109]

Hughes, A. The topography of vision in mammals of contrasting lifestyles: comparative optics and retinal organisation. Springer-Verlag Berlin. 1977.

Johnson, GL. Contributions to the comparative anatomy of the mammalian eye, chiefly based on ophthalmoscopic examination. Vol. 194. Philosophical transactions of the Royal Society of London; (London): 1901. p. 1-82.Series B: Biological Sciences

Kaas JH. Serendipity and the Siamese cat: the discovery that genes for coat and eye pigment affect the brain. Ilar J. 2005; 46:357–63. [PubMed: 16179744]

Karakousis PC, John SK, Behling KC, Surace EM, Smith JE, Hendrickson A, Tang WX, Bennett J, Milam AH. Localization of pigment epithelium derived factor (PEDF) in developing and adult human ocular tissues. Molecular Vision. 2001; 7:154–63. [PubMed: 11438800]

Ke K, Xia C, Islam MN, Welsh MJ, Freeman MJ. Mid-infrared absorption spectroscopy and differential damage in vitro between lipids and proteins by an all-fiber-integrated supercontinuum laser. Optics express. 2009; 17:12627–40. [PubMed: 19654667]

Kelly JP, Weiss AH. Topographical retinal function in oculocutaneous albinism. Am J Ophthalmol. 2006; 141:1156–8. [PubMed: 16765699]

Kim DY, Fingler J, Werner JS, Schwartz DM, Fraser SE, Zawadzki RJ. In vivo volumetric imaging of human retinal circulation with phase-variance optical coherence tomography. Biomed Opt Express. 2011; 2:1504–13. [PubMed: 21698014]

Kinnear PE, Jay B, Witkop CJ Jr. Albinism. Surv Ophthalmol. 1985; 30:75–101. [PubMed: 3934778]

Kirby ML, Galea M, Loane E, Stack J, Beatty S, Nolan JM. Foveal anatomic associations with the secondary peak and the slope of the macular pigment spatial profile. Invest Ophthalmol Vis Sci. 2009; 50:1383–91. [PubMed: 18936143]

Knighton RW, Gregori G, Budenz DL. Variance reduction in a dataset of normal macular ganglion cell plus inner plexiform layer thickness maps with application to glaucoma diagnosis. Invest Ophthalmol Vis Sci. 2012; 53:3653–61. [PubMed: 22562512]

Kozulin P, Natoli R, Bumsted O'Brien KM, Madigan MC, Provis JM. The Cellular Expression of Antiangiogenic Factors in Fetal Primate Macula. Invest. Ophthalmol. Vis. Sci. 2010; 51:4298–306. [PubMed: 20357200]

Kozulin P, Natoli R, Madigan MC, O'Brien KM, Provis JM. Gradients of Eph-A6 expression in primate retina suggest roles in both vascular and axon guidance. Mol Vis. 2009a; 15:2649–62. [PubMed: 20011078]

Kozulin P, Natoli R, O'Brien KM, Madigan MC, Provis JM. Differential expression of anti-angiogenic factors and guidance genes in the developing macula. Mol Vis. 2009b; 15:45–59. [PubMed: 19145251]

Labin AM, Ribak EN. Retinal glial cells enhance human vision acuity. Physical review letters. 2010; 104:158102. [PubMed: 20482021]

Lambot MA, Depasse F, Noel JC, Vanderhaeghen P. Mapping labels in the human developing visual system and the evolution of binocular vision. J Neurosci. 2005; 25:7232–7. [PubMed: 16079405]

Lee KA, King RA, Summers CG. Stereopsis in patients with albinism: clinical correlates. J AAPOS. 2001; 5:98–104. [PubMed: 11304818]

Levi DM, Klein SA, Yap YL. Positional uncertainty in peripheral and amblyopic vision. Vision Res. 1987; 27:581–97. [PubMed: 3660620]

Li KY, Tiruveedhula P, Roorda A. Intersubject variability of foveal cone photoreceptor density in relation to eye length. Invest Ophthalmol Vis Sci. 2010; 51:6858–67. [PubMed: 20688730]

Li Y, Wolf E. Focal shifts in diffracted converging spherical waves. Optics comm. 1981; 39:211–15.

Magitot MA. Etude sur le développement de la rétine humaine. Annales d'Occulistique. 1910; 143:241–82.

Maldonado RS, O'Connell RV, Sarin N, Freedman SF, Wallace DK, Cotten CM, Winter KP, Stinnett S, Chiu SJ, Izatt JA, Farsiu S, Toth CA. Dynamics of human foveal development after premature birth. Ophthalmology. 2011; 118:2315–25. [PubMed: 21940051]

Mann, I. The Development of the Human Eye. Second edition. Grune and Stratton New York: 1928. 1964

Marmor MF, Choi SS, Zawadzki RJ, Werner JS. Visual insignificance of the foveal pit: reassessment of foveal hypoplasia as fovea plana. Arch Ophthalmol. 2008; 126:907–13. [PubMed: 18625935]

McAllister JT, Dubis AM, Tait DM, Ostler S, Rha J, Stepien KE, Summers CG, Carroll J. Arrested development: high-resolution imaging of foveal morphology in albinism. Vision Res. 2010; 50:810–7. [PubMed: 20149815]

McGuire DE, Weinreb RN, Goldbaum MH. Foveal hypoplasia demonstrated in vivo with optical coherence tomography. Am J Ophthalmol. 2003; 135:112–4. [PubMed: 12504716]

McLaughlin T, Hindges R, O'Leary DD. Regulation of axial patterning of the retina and its topographic mapping in the brain. Curr Opin Neurobiol. 2003a; 13:57–69. [PubMed: 12593983]

McLaughlin T, Torborg CL, Feller MB, O'Leary DD. Retinotopic map refinement requires spontaneous retinal waves during a brief critical period of development. Neuron. 2003b; 40:1147–60. [PubMed: 14687549]

Merino D, Duncan JL, Tiruveedhula P, Roorda A. Observation of cone and rod photoreceptors in normal subjects and patients using a new generation adaptive optics scanning laser ophthalmoscope. Biomed Opt Express. 2011; 2:2189–201. [PubMed: 21833357]

Miglior S, Brigatti L, Velati P, Balestreri C, Rossetti L, Bujtar E, Orzalesi N. Relationship between morphometric optic disc parameters, sex and axial length. Curr Eye Res. 1994; 13:119–24. [PubMed: 8194358]

Miller DT, Williams DR, Morris GM, Liang J. Images of cone photoreceptors in the living human eye. Vision Res. 1996; 36:1067–79. [PubMed: 8762712]

Mintz-Hittner HA, Knight-Nanan DM, Satriano DR, Kretzer FL. A small foveal avascular zone may be an historic mark of prematurity. Ophthalmology. 1999; 106:1409–13. [PubMed: 10406630]

Nag TC, Wadhwa S, Alladi PA, Sanyal T. Localization of 4-hydroxy 2-nonenal immunoreactivity in aging human retinal Muller cells. Ann Anat. 2011; 193:205–10. [PubMed: 21454059]

Nolan JM, Stringham JM, Beatty S, Snodderly DM. Spatial profile of macular pigment and its relationship to foveal architecture. Invest Ophthalmol Vis Sci. 2008; 49:2134–42. [PubMed: 18436846]

Nusinowitz S, Sarraf D. Retinal function in X-linked ocular albinism (OA1). Curr Eye Res. 2008; 33:789–803. [PubMed: 18798082]

Oetting WS, Summers CG, King RA. Albinism and the associated ocular defects. Metab Pediatr Syst Ophthalmol. 1994; 17:5–9. [PubMed: 8719278]

Oliver MD, Dotan SA, Chemke J, Abraham FA. Isolated foveal hypoplasia. Br J Ophthalmol. 1987; 71:926–30. [PubMed: 3427001]

Pfeiffenberger C, Cutforth T, Woods G, Yamada J, Renteria RC, Copenhagen DR, Flanagan JG, Feldheim DA. Ephrin-As and neural activity are required for eye-specific patterning during retinogeniculate mapping. Nat Neurosci. 2005; 8:1022–7. [PubMed: 16025107]

Polyak, SL. The Retina. The University of Chicago Press; 1941.

Popovic Z, Knutsson P, Thaung J, Owner-Petersen M, Sjostrand J. Noninvasive imaging of human foveal capillary network using dual-conjugate adaptive optics. Invest Ophthalmol Vis Sci. 2011; 52:2649–55. [PubMed: 21228372]

Provis JM. The distribution and size of ganglion cells in the retina of the pigmented rabbit: A quantitative analysis. Journal of Comparative Neurology. 1979; 185:121–38. [PubMed: 429611]

Provis JM. Development of the primate retinal vasculature. Prog Retin Eye Res. 2001; 20:799–821. [PubMed: 11587918]

Provis JM, Diaz CM, Dreher B. Ontogeny of the primate fovea: a central issue in retinal development. Progress in Neurobiology. 1998; 54:549–80. [PubMed: 9550191]

Provis JM, Hendrickson AE. The foveal avascular region of developing human retina. Arch Ophthalmol. 2008; 126:507–11. [PubMed: 18413520]

Provis JM, Penfold PL, Cornish EE, Sandercoe TM, Madigan MC. Anatomy and development of the macula: specialisation and the vulnerability to macular degeneration. Clin Exp Optom. 2005; 88:269–81. [PubMed: 16255686]

Provis JM, Sandercoe T, Hendrickson AE. Astrocytes and blood vessels define the foveal rim during primate retinal development. Investigative Ophthalmology & Visual Science. 2000; 41:2827–36. [PubMed: 10967034]

Putnam NM, Hofer HJ, Doble N, Chen L, Carroll J, Williams DR. The locus of fixation and the foveal cone mosaic. J Vis. 2005; 5:632–9. [PubMed: 16231998]

Reichenbach, A.; Bringmann, A. Müller cells in the healthy and diseased retina. Spinger New York: 2010.

Rodieck, RW. Comparative Primate Biology. Vol 4: Neurosciences. Alan R. Liss, Inc; 1988. The Primate Retina; p. 203-78.

Rohen JW, Castenholtz A. Über die Zentralisation der Retina bei Primaten. Folia Primatologica. 1967; 5:92–147.

Roorda A, Romero-Borja F, Donnelly Iii W, Queener H, Hebert T, Campbell M. Adaptive optics scanning laser ophthalmoscopy. Opt Express. 2002; 10:405–12. [PubMed: 19436374]

Roorda A, Williams DR. Optical fiber properties of individual human cones. Journal of vision. 2002; 2:404–12. [PubMed: 12678654]

Rossi EA, Chung M, Dubra A, Hunter JJ, Merigan WH, Williams DR. Imaging retinal mosaics in the living eye. Eye (Lond). 2011; 25:301–8. [PubMed: 21390064]

Rossi EA, Roorda A. The relationship between visual resolution and cone spacing in the human fovea. Nat Neurosci. 2010; 13:156–7. [PubMed: 20023654]

Rynders MC, Grosvenor T, Enoch JM. Stability of the Stiles-Crawford function in a unilateral amblyopic subject over a 38-year period: a case study. Optometry and vision science : official publication of the American Academy of Optometry. 1995; 72:177–85. [PubMed: 7609940]

Schmolesky MT, Wang Y, Creel DJ, Leventhal AG. Abnormal retinotopic organization of the dorsal lateral geniculate nucleus of the tyrosinase-negative albino cat. J Comp Neurol. 2000; 427:209–19. [PubMed: 11054689]

Schulze-Dobold C, Sharpe LT, Jagle H. Photoreceptor directional sensitivity in normals, dichromats and S-cone monochromats. J Modern Optics. 2009; 56:2189–202.

Seo JH, Yu YS, Kim JH, Choung HK, Heo JW, Kim SJ. Correlation of visual acuity with foveal hypoplasia grading by optical coherence tomography in albinism. Ophthalmology. 2007; 114:1547–51. [PubMed: 17337060]

Shewan D, Dwivedy A, Anderson R, Holt CE. Age-related changes underlie switch in netrin-1 responsiveness as growth cones advance along visual pathway. Nat Neurosci. 2002; 5:955–62. [PubMed: 12352982]

Silveira LC, Perry VH, Yamada ES. The retinal ganglion cell distribution and the representation of the visual field in area 17 of the owl monkey, Aotus trivirgatus. Vis Neurosci. 1993; 10:887–97. [PubMed: 8217938]

Snyder, AW. `Photoreceptor optics - theoretical principles.'. In: A.W.M. Snyder, R., editor. Photorecptor optics. Heidelberg: Springer-Verlag: 1975. p. 38-55.

Snyder AW, Laughlin SB, Stavenga DG. Information capacity of eyes. Vision Res. 1977; 17:1163–75. [PubMed: 595380]

Song H, Chui TY, Zhong Z, Elsner AE, Burns SA. Variation of cone photoreceptor packing density with retinal eccentricity and age. Invest Ophthalmol Vis Sci. 2011; 52:7376–84. [PubMed: 21724911]

Sonoda S, Isashiki Y, Tabata Y, Kimura K, Kakiuchi T, Ohba N. A novel PAX6 gene mutation (P118R) in a family with congenital nystagmus associated with a variant form of aniridia. Graefes Arch Clin Exp Ophthalmol. 2000; 238:552–8. [PubMed: 10955655]

Spaide RF, Curcio CA. Anatomical correlates to the bands seen in the outer retina by optical coherence tomography: literature review and model. Retina. 2011; 31:1609–19. [PubMed: 21844839]

Sparrow JR, Ueda K, Zhou J. Complement dysregulation in AMD: RPE-Bruch's membrane-choroid. Molecular Aspects of Medicine. 2012; 33:436–45. [PubMed: 22504022]

Spranger J, Osterhoff M, Reimann M, Mohlig M, Ristow M, Francis MK, Cristofalo V, Hammes HP, Smith G, Boulton M, Pfeiffer AF. Loss of the antiangiogenic pigment epithelium-derived factor in patients with angiogenic eye disease. Diabetes. 2001; 50:2641–5. [PubMed: 11723044]

Springer A, Hendrickson A. Development of the primate area of high acuity.1. Use of finite element analysis models to identify mechanical variables affecting pit formation. Visual Neuroscience. 2004a; 21:53–62. [PubMed: 15137581]

Springer A, Hendrickson A. Development of the primate area of high acuity. 2. Quantitative morphological changes associated with retinal and pars plana growth. Visual Neuroscience. 2004b; 21:775–90. [PubMed: 15683563]

Springer AD. New role for the primate fovea: a retinal excavation determines photoreceptor deployment and shape. Visual Neuroscience. 1999; 16:629–36. [PubMed: 10431912]

Springer AD, Hendrickson AE. Development of the primate area of high acuity, 3: temporal relationships between pit formation, retinal elongation and cone packing. Vis Neurosci. 2005; 22:171–85. [PubMed: 15935110]

Springer AD, Troilo D, Possin D, Hendrickson AE. Foveal cone density shows a rapid postnatal maturation in the marmoset monkey. Vis Neurosci. 2011; 28:473–84. [PubMed: 22192504]

Stavenga DG. Angular and spectral sensitivity of fly photoreceptors. I. Integrated facet lens and rhabdomere optics. Journal of comparative physiology. A, Neuroethology, sensory, neural, and behavioral physiology. 2003; 189:1–17.

Stellmach, V.; Crawford, SE.; Zhou, W.; Bouck, N. Prevention of ischemia-induced retinopathy by the natural ocular antiangiogenic agent pigment epithelium-derived factor.[see comment]; Proceedings of the National Academy of Sciences of the United States of America; 2001. p. 2593-7.

Stone J. The number and distribution of ganglion cells in the cat's retina. Journal of Comparative Neurology. 1978; 180:753–72. [PubMed: 681546]

Stone J, Johnston E. The topography of primate retina: a study of the human, bushbaby, and new- and old-world monkeys. Journal of Comparative Neurology. 1981; 196:205–23. [PubMed: 7217355]

Summers CG. Vision in albinism. Trans Am Ophthalmol Soc. 1996; 94:1095–155. [PubMed: 8981720]

Tam J, Martin JA, Roorda A. Noninvasive visualization and analysis of parafoveal capillaries in humans. Invest Ophthalmol Vis Sci. 2010; 51:1691–8. [PubMed: 19907024]

Tam J, Roorda A. Speed quantification and tracking of moving objects in adaptive optics scanning laser ophthalmoscopy. J Biomed Opt. 2011; 16:036002. [PubMed: 21456866]

Tancred E. The distribution and sizes of ganglion cells in the retinas of five Australian marsupials. The Journal of Comparative Neurology. 1981; 196:585–603. [PubMed: 7204673]

Tick S, Rossant F, Ghorbel I, Gaudric A, Sahel JA, Chaumet-Riffaud P, Paques M. Foveal shape and structure in a normal population. Invest Ophthalmol Vis Sci. 2011; 52:5105–10. [PubMed: 21803966]

Trieschmann M, van Kuijk FJ, Alexander R, Hermans P, Luthert P, Bird AC, Pauleikhoff D. Macular pigment in the human retina: histological evaluation of localization and distribution. Eye. 2008; 22:132–7. [PubMed: 17401321]

Vajzovic L, Hendrickson A, O'Connell RV, Clark LA, Tran-Viet D, Possin D, Chiu SJ, Farsiu S, Toth CA. Maturation of the Human Fovea: Correlation of Spectral-Domain Optical Coherence Tomography Findings with Histology. Am J Ophthalmol. 2012; 154:779–89 e2. [PubMed: 22898189]

Van Essen. A tension-based theory of morphogenesis and compact wiring in the central nervous system. Nature. 1997; 385:313–18. [PubMed: 9002514]

Wagner-Schuman M, Dubis AM, Nordgren RN, Lei Y, Odell D, Chiao H, Weh E, Fischer W, Sulai Y, Dubra A, Carroll J. Race- and sex-related differences in retinal thickness and foveal pit morphology. Invest Ophthalmol Vis Sci. 2011; 52:625–34. [PubMed: 20861480]

Walls GL. Significance of the foveal depression. Archives of Ophthalmology. 1937; 18:912–19.

Wandell, B. Foundations of Vision. Sinauer Associates Sunderland; Massachusettes: 1995.

Wang J, Spencer R, Leffler JN, Birch EE. Critical period for foveal fine structure in children with regressed retinopathy of prematurity. Retina. 2012; 32:330–9. [PubMed: 21900854]

Wang Q, Kocaoglu OP, Cense B, Bruestle J, Jonnal RS, Gao W, Miller DT. Imaging retinal capillaries using ultrahigh-resolution optical coherence tomography and adaptive optics. Invest Ophthalmol Vis Sci. 2011; 52:6292–9. [PubMed: 21245397]

Weale RA. Why does the human retina possess a fovea? Nature. 1966; 212:255–56. [PubMed: 4961475]

Webb SV, Kaas JH. The sizes and distribution of ganglion cells in the retina of the owl monkey, *Aotes trivirgatus*. Vision Research. 1976; 16:1247–54. [PubMed: 827113]

Wexler A, Tor B, Elsas T. Macular thickness measurements in helathy Norwegian volunteers: an optical coherence tomography study. BMC Ophthalmology. 2010; 10:13. [PubMed: 20465801]

Weymouth FW, Hines DC, Acres LH, Raaf JE, Wheeler MC. Visual Acuity Within the Area Centralis and its Relation to Eye Movements and Fixation. American Journal of Ophthalmology. 1928; 11:947–60.

Williams DR. Visual consequences of the foveal pit. Invest Ophthalmol Vis Sci. 1980; 19:653–67. [PubMed: 7380624]

Wilson HR, Mets MB, Nagy SE, Kressel AB. Albino spatial vision as an instance of arrested visual development. Vision Res. 1988; 28:979–90. [PubMed: 3254652]

Wolin, LR.; Massopust, LC. Morphology of the primate retina. In: Noback, CR.; Montagna, W., editors. The Primate Brain. Vol. Vol. 1. Appleton-Century-Crofts; New York: 1970. p. 1-27.

Woollard, HH. The differentiation of the retina in primates; Proceedings of the Zoological Society of London; 1927. p. 1-18.

Yamada E. Some structural features of the fovea centralis in the human retina. Archives of Ophthalmology. 1969; 82:151–59. [PubMed: 4183671]

Yanni SE, Wang J, Chan M, Carroll J, Farsiu S, Leffler JN, Spencer R, Birch EE. Foveal avascular zone and foveal pit formation after preterm birth. Br J Ophthalmol. 2012; 96:961–6. [PubMed: 22544530]

Yu DY, Cringle SJ, Su EN. Intraretinal oxygen distribution in the monkey retina and the response to systemic hyperoxia. Invest Ophthalmol Vis Sci. 2005; 46:4728–33. [PubMed: 16303972]

Yuodelis C, Hendrickson A. A qualitative and quantitative analysis of the human fovea during development. Vision Research. 1986; 26:847–55. [PubMed: 3750868]

Zeffren BS, Applegate RA, Bradley A, van Heuven WA. Retinal fixation point location in the foveal avascular zone. Invest Ophthalmol Vis Sci. 1990; 31:2099–105. [PubMed: 2211007]

Zhang Y, Rha J, Jonnal R, Miller D. Adaptive optics parallel spectral domain optical coherence tomography for imaging the living retina. Opt Express. 2005; 13:4792–811. [PubMed: 19495398]

Zheng Y, Gandhi JS, Stangos AN, Campa C, Broadbent DM, Harding SP. Automated segmentation of foveal avascular zone in fundus fluorescein angiography. Invest Ophthalmol Vis Sci. 2010; 51:3653–9. [PubMed: 20130279]

Highlights

The *fovea centralis* forms in an avascular zone (FAZ) defined by molecular factors FAZ size, and shape of the fovea, is determined by genetic and environmental cues Presence of midget circuitry in central retina facilitates formation of the fovea Narrowing and elongation of cones is a key adaptation that enhances acuity Cones differentiate narrow, elongated shapes even when a fovea is absent

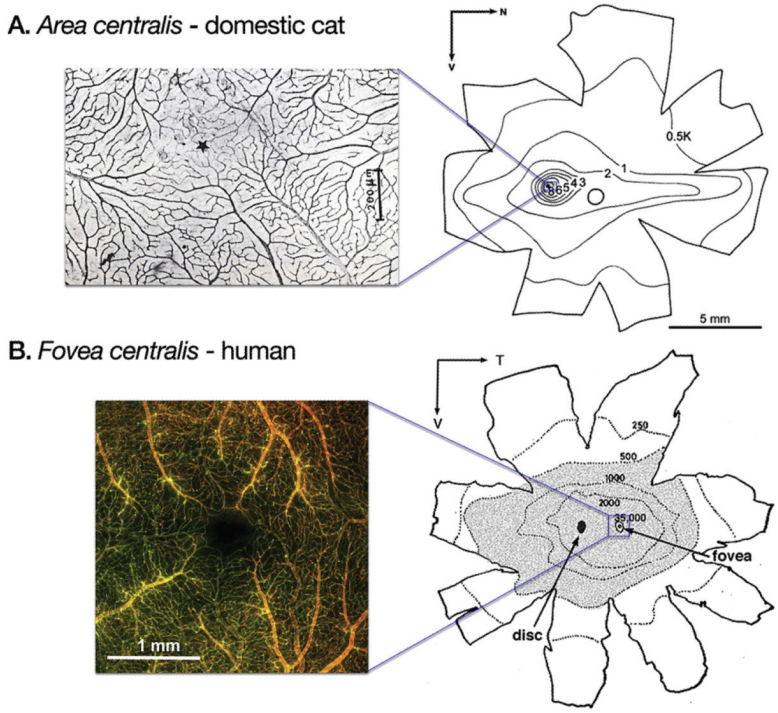

Figure 1.

Vascular and neuronal adaptations at the *area centralis* of the cat retina, and at the *fovea centralis* of the human retina. **A:** The image shows the appearance of the retinal vasculature at the area centralis of the cat retina. The map shows ganglion cell isodensity lines in the cat retina (/mm^2) Adapted, with permission http://www.retinalmaps.com.au/. Retinal vessels converge on the *area centralis* (star) which is supplied by a network of capillaries; large diameter vessels do not cross the specialized area, where peak is ganglion cell density ~8K cells/mm^2. **B:** The image shows the arrangement of vessels at the *fovea centralis* of the human retina (courtesy of Prof Dao-Yi Yu, University of Western Australia). Large vessels converge on the foveal avascular zone (centre), and give rise to a dense microvascular network that supplies the macular region. The map shows the ganglion cell topography in a human retina. While ganglion cells are absent from the central fovea (corresponding with with the avascular area), they reach a maximum density of ~35K/mm^2 on the foveal rim (see Curcio & Allen (1990) *J. Comp. Neurol.*). The shading indicates the region where ganglion cell density is elevated, resulting in a `visual streak'-like feature in the retina (adapted from Stone and Johnson (1981) *J. Comp. Neurol.*).

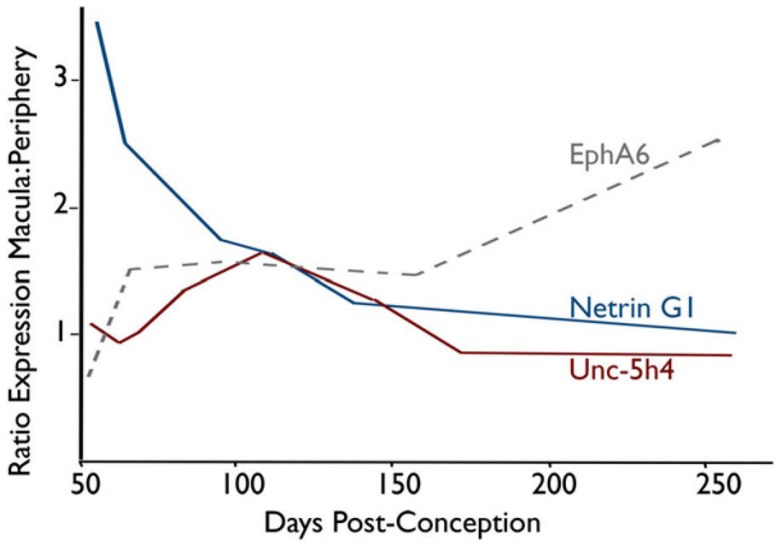

Figure 2.

Relative levels of expression of 3 guidance factors in the macula of macaque monkey retina during prenatal and early postnatal development. Both Netrin G1 and Unc-5h4 mRNAs tend to be uniformly distributed across the retina in late development and post-natal. However, expression of EphA6 continues to rise at the macula after birth (~174 dPC), suggesting that it may be playing a role in defining synaptic territories in the brain in the postnatal period.

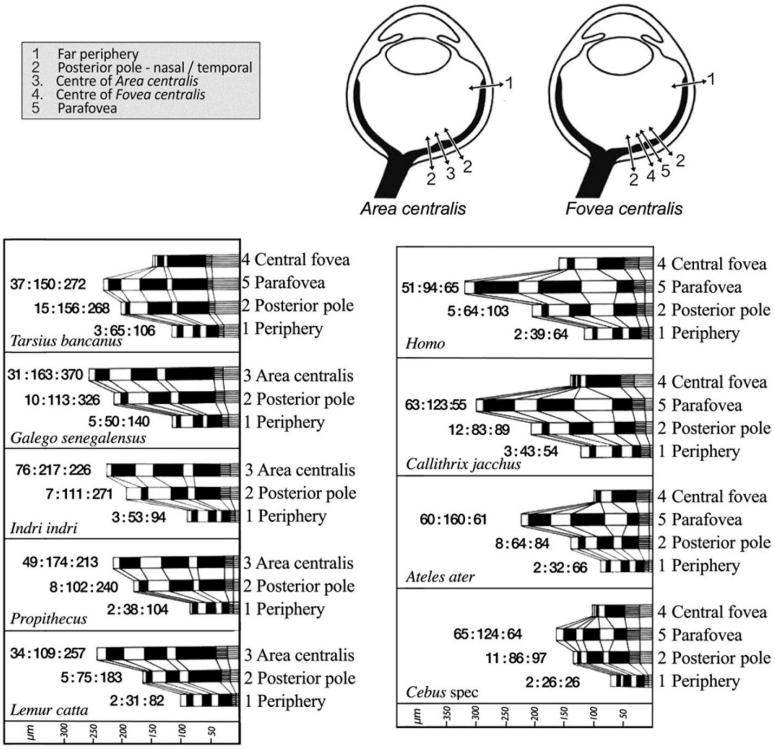

Figure 3.

Representative examples from the semi-quantitative analyses of retinal cell densities in primate retinas (redrawn and modified from Figures 1, 3 and 4 of Rohen & Castenholz (1967)). Five standard retinal sample locations are indicated in the upper drawings. Retinal thickness is represented in the lower diagrams by horizontal bars, drawn to scale (bottom of the diagram). The thickness of each layer, and the lengths of the inner and outer segments, is indicated by the striped segments, at the right-hand end of each histogram; black bands indicate the thickness of the cellular layers (outer nuclear (ONL), inner nuclear (INL) and ganglion cell layers (GCL), from right to left); white bands represent the intervening plexiform layers, and the nerve fibre layer (left-hand end of each histogram). The numbers show the ratios of cells in the cell layers at each location (GC:INL:ONL). The illustration shows that in all cases, the photoreceptors at the posterior pole are significantly elongated compared to the periphery. In *Galego senegalensis*, the photoreceptors in the *area centralis* (location 3) are almost twice the length of photoreceptor segments in the periphery. The data indicate that a fovea is not required to generate photoreceptor elongation, and hence packing, of central photoreceptors.

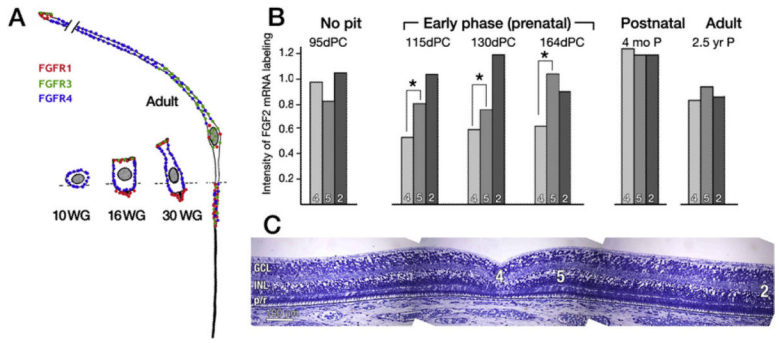

Figure 4.

Fibroblast growth factor (FGF)-2 and FGF receptor (R)1, R3 and R4 mRNA expression during morphological development of cones. **A:** The changing morphology of foveal cones during fetal life, compared with an adult cone is shown including the typical distribution of three FGFRs at four different stages (adapted from Hendrickson, 1984). **B:** Histograms showing the levels of expression of the morphogenetic growth factor, FGF2 by cones 3 retinal locations at 5 timepoints. The locations are numbered for comparison with Fig 3 – `4', Fovea; `5' Parafovea; `2', Posterior pole (nasal side). The data show that FGF2 is expressed at high levels in foveal cones before (95dPC) and after (4mo postnatal) formation of the fovea, but not during (105dPC to birth). Asterisks indicate a significant difference in the level of FGF2 expressed. During early formation of the fovea, *in utero*, cones are slow to elongate and have low levels of FGF2 mRNA. After birth they elongate rapidly, and express high levels of FGF2. **C:** Section through a macaque fovea at 150dPC, indicating the 3 locations (4, 5 and 2) where FGF2 expression was measured, to generate the histograms. Note that cones on the edge of the fovea (5), which express high levels of FGF2, are considerably more elongated than those in the central fovea, which express significantly lower levels of FGF2. INL, inner nuclear layer; GCL, ganglion cell layer; p/r photoreceptors; dPC days post conception.

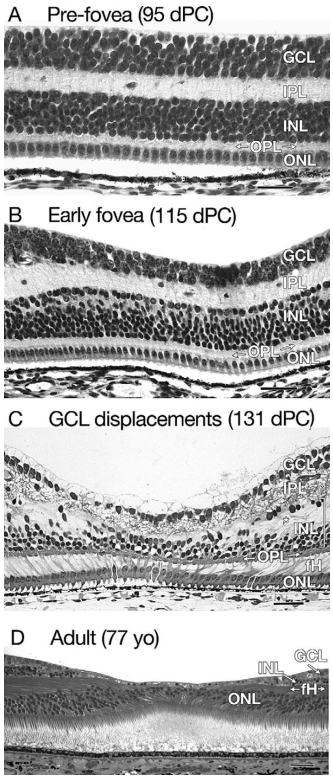

Figure 5.

Excavation of the fovea during development(macaque, A–C), and in the mature fovea in a 77 year old human donor (D). **A:** Before the fovea forms, the location of the future fovea can be identified by the predominance of cones, seen as a single layer of cuboidal cells in the ONL. The GCL comprises many layers of ganglion cell bodies. **B.** In the very early fovea the GCL is thinner than at 95 dPC, but the depth of the other retinal layers is virtually unchanged. **C:** Ganglion cells are displaced from the early fovea very quickly, so that within a short period of time the GCL comprises only one layer of cells, as seen here. Morphological evidence of displacement includes the outward angling of the axons of cones forming the layer of Henle fibres, except those in the fovea. In addition, processes of bipolar cells can be seen obliquely crossing the transient layer of Chievitz (*), to synapse on their target ganglion cells that have been centrifugally displaced. **D.** In the adult fovea there are very few ganglion cells present centrally, and cone cell bodies lie close to the surface of the retina. The elongated inner and outer segments constitute more than 50% of the retinal thickness within the fovea. INL, inner nuclear layer; IPL, inner plexiform layer; fH, fibres of Henle; GCL, ganglion cell layer; ONL, outer nuclear layer; OPL, outer plexiform layer; p/r photoreceptors; dPC days post conception. Scale bars represent 50 μm.

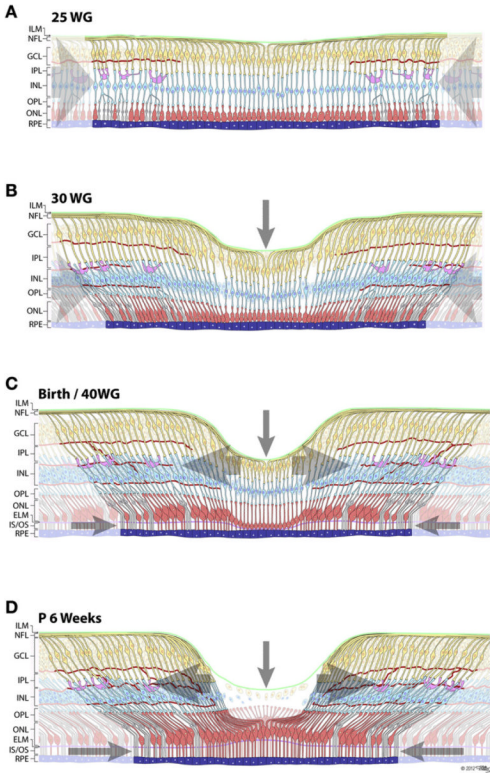

Figure 6.

Diagrammatic representation of four stages in development of the fovea. Ages are an approximate indication of stages of human development. Cones are shown in red, rods in grey, bipolar cells in blue, amacrine cells in pink, and ganglion cells in yellow. The relationships between cells in the different layers approximates the midget circuits in the retina. Red lines represent the approximate arrangements of the retinal vessels. **A:** Indicating the appearance of the central macula just prior to the early appearance of the fovea. Retinal vessels are present only in the GCL, and the GCL comprises several layers of cells. At this stage cells in all layers tend to crowd toward the incipient fovea (centripetal displacement), as indicated by the large grey arrows. Photoreceptors on the edge of the foveal cone mosaic (where rods are absent) are more elongated than those in the centre. **B:** Once the FAZ is defined, the inner surface of the retina within the FAZ is deformed, forming a shallow depression, which is the first indication of formation of the fovea. The force that deforms the retina within the FAZ seems likely to be intraocular pressure. Centripetal displacement of cells in the outer layers of the retina continues, as indicated by the large grey arrows. Cones outside the fovea are narrower and more elongated than those within the developing fovea. **C:** By birth the GCL is significantly reduced in thickness, due to the centrifugal displacement of ganglion cells (indicated by arrows in the inner retina). However, all cell layers are present within the fovea at birth. Retinal vessels are present in the INL, although anatomosis between the layers is not complete. Cones on the foveal rim are significantly elongated, the cell bodies are stacked, and their inner segments are distinct. Cones in the fovea remain in a monolayer, are less elongated and have only rudimentary inner and outer segments. **D:** In the first few weeks postnatal, cones in the central fovea differentiate rapidly so that by 1–2 months the central cones are more elongated and have longer axons (fibres of Henle) than those on the edge of the fovea (compare with C). Ganglion cells, bipolar cells and the synaptic pedicles of cones have been displaced from the central fovea. The perifoveal capillaries have formed an anastomosis around the fovea. The mature form of the

fovea (not shown - see Fig 5D) continues to develop over a period of many months, and includes further centripetal displacement of photoreceptors (increasing photoreceptor density in the foveola), continued centrifugal displacement of bipolar and ganglion cells, and morphological remodeling of the shape of the depression. INL, inner nuclear layer; ILM, inner limiting membrane; IPL, inner plexiform layer; ELM, external limiting membrane; fH, fibres of Henle; GCL, ganglion cell layer; NFL, nerve fibre layer; ONL, outer nuclear layer; OPL, outer plexiform layer; P, postnatal; RPE, retinal pigmented epiltheilum; WG, weeks' gestation.

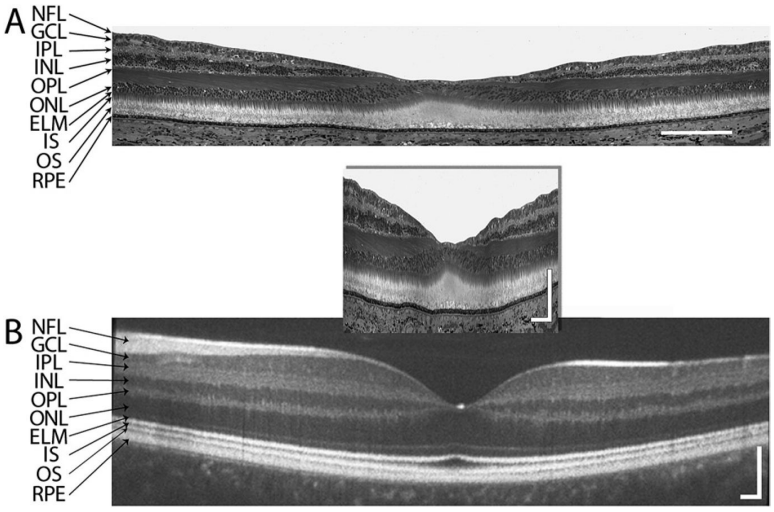

Figure 7.

A comparison of histological and OCT images of the cross-sectional appearance of the human retina, at the fovea centralis. **A:** Histological section of an adult retina (77 years old), showing the layers of the retina. **B:** SDOCT imaging of a 28 year old subject. The inset shows the same histological image (A) on the same scale as the SDOCT image (aspect ratio 1 : 2.8). Abbreviations: NFL, nerve fiber layer; GCL, ganglion cell layer; IPL, inner plexiform layer; INL, inner nuclear layer; OPL, outer plexiform layer; FAZ, foveal avascular zone; HFL, Henle fiber layer; ONL, outer nuclear layer; ELM, external limiting membrane; IS, inner segment; OS, outer segment; RPE, retinal pigmented epithelium. Scale bars represent 200 μm.

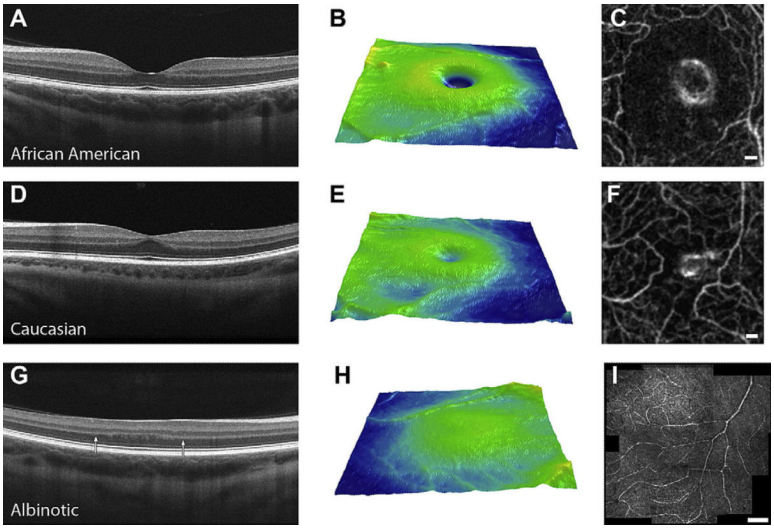

Figure 8.

The different morphologies of the fovea and foveal avascular zones in three individuals. The left column shows the retina in cross section (B-scan); the middle column is a 3D macular thickness plot; the right hand column shows vessels in the central macula, obtained by fluorescein angiography. **A, B:** A broad and deep fovea is typically seen in individuals of African American descent. **C:** The FAZ of the same subject is ~800–1000 μm in diameter. **D, E:** The shallow fovea of a Caucasian subject that is associated (**F)** with a smaller FAZ. **G, H:** An albinotic subject who lacks a *fovea*, and **(I)** also lacks a foveal avascular area. Note that the central photoreceptors are elongated in the central area (between the arrows), despite the absence of the fovea. Scale bars represents 100 μm.

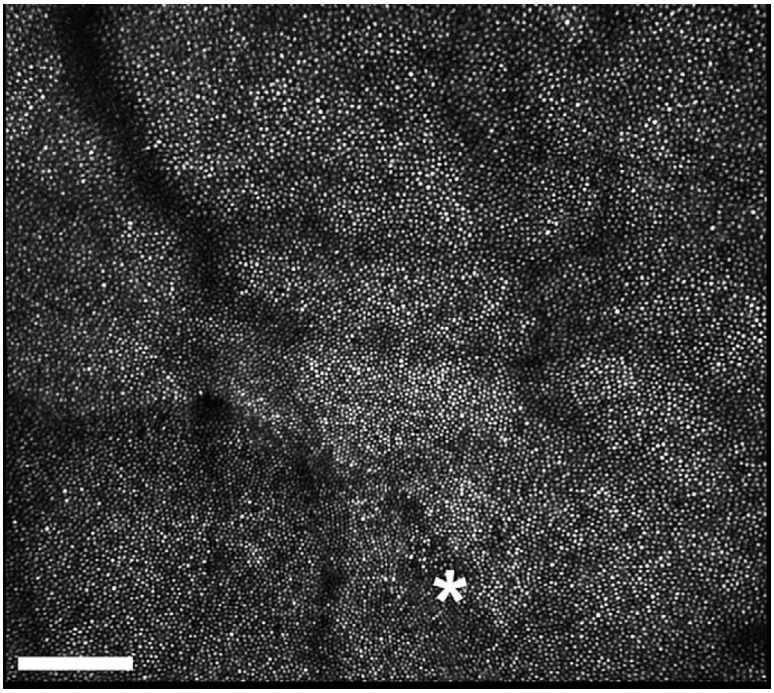

Figure 9.

An example of an AOSLO image of the photoreceptor mosaic, from the same albinotic individual as illustrated in Fig 8 (G–I). Peak cone density in this individual was at the lower end of the normal range (97,182 cones/mm^2). The image shows evidence of a narrowing of apertures in the cluster of cones seen just below the center of the image, and just above the fixation point (indicated by the asterisk). Scale bar represents 100 μm.

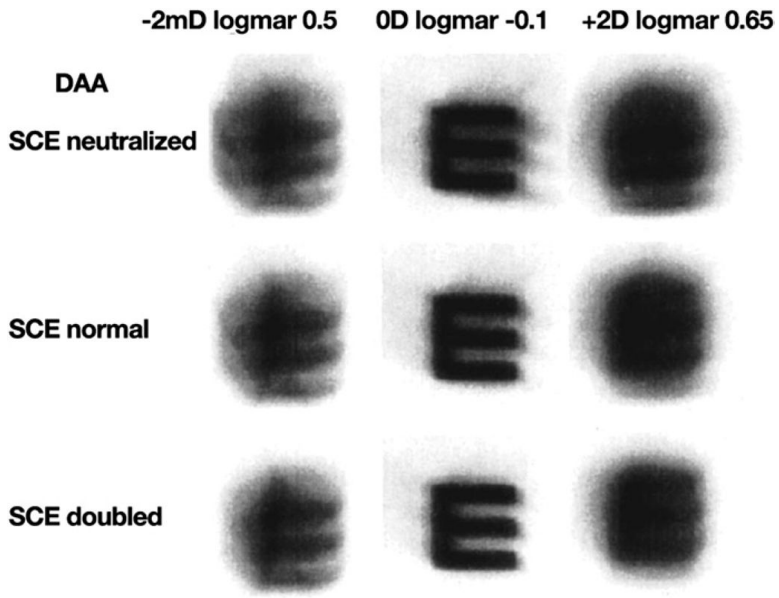

Figure 10.

Effect of apodizing a 6 mm pupil by the Stiles Crawford effect. The central photo shows the normal retinal appearance of a 0.1 logmar letter `E'. The manipulations include ±2D of defocus and neutralising (top row) or doubling the apodization (bottom row). The SC-effect also appears to give some tolerance to myopic defocus. Reproduced with permission from Atchison et al., 2002.

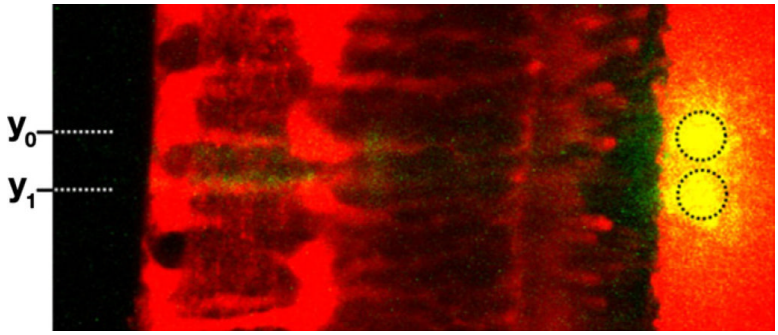

Figure 11.
The progress of two narrow laser beams placed at y_0 and y_1 traversing a guinea pig retina along Müller cell processes, and forming two reasonably well resolved spot of light at the photoreceptor level (to the right). Reproduced with permission from Agte et al., 2011

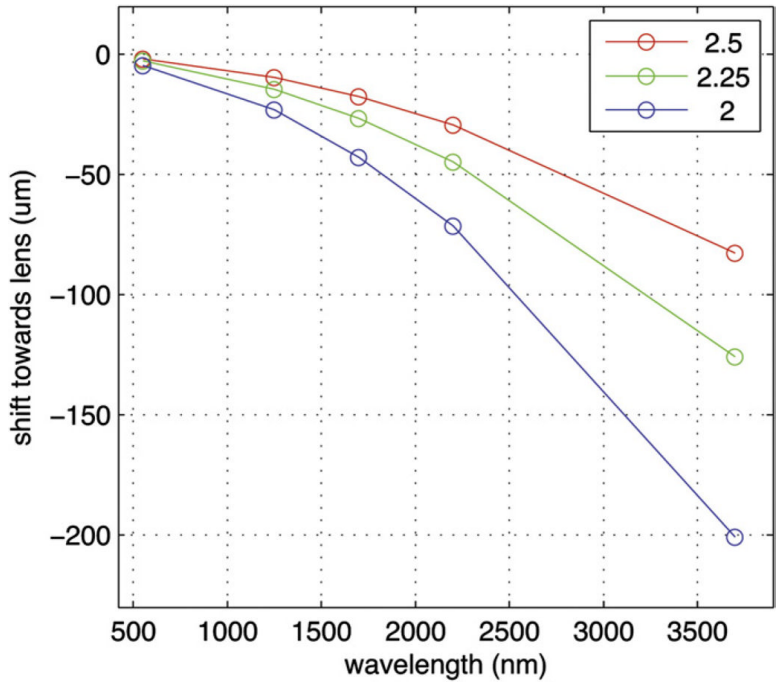

Figure 12.

Plot showing the locations the four `windows' of infrared transmission (open circles) in relation to shifts of the focal point, as a function of wavelength, for 3 pupil diameters (2, 2.25 and 2.5 mm). When the pupil diameter is near in size to the wavelength (or if the focal length is very long), diffraction operates to move the axial focal point closer to the lens, compared to the expectation for geometric optics (quantified by the Fresnel number).